

Probing the speed of gravity with LVK, LISA, and joint observations

Ian Harry^{1,*} and Johannes Noller^{1,2,†}

¹*Institute of Cosmology & Gravitation, University of Portsmouth, Portsmouth, PO1 3FX, U.K.*

²*DAMTP, University of Cambridge, Wilberforce Road, Cambridge CB3 0WA, U.K.*

(Dated: October 25, 2022)

Theories of dark energy that affect the speed of gravitational waves c_{GW} on cosmological scales naturally lead to a frequency-dependent transition of that speed close to the LIGO/Virgo/KAGRA (LVK) band. While observations such as GW170817 assure us that c_{GW} is extremely close to the speed of light in the LVK band, a frequency-dependent transition below the LVK band is a smoking-gun signal for large classes of dynamical dark energy theories. Here we discuss 1) how the remnants of such a transition can be constrained with observations in the LVK band, 2) what signatures are associated with such a transition in the LISA band, and 3) how joint observations in the LVK and LISA bands allow us to place tight constraints on this transition and the underlying theories. We find that deviations of c_{GW} can be constrained down to a level of $\sim 10^{-17}$ in the LVK and LISA bands even for mild frequency-dependence, much stronger than existing bounds for frequency-independent $c_{\text{GW}} \neq c$. We use the strain data from GW170817 to bound the deviation of c_{GW} to be less than 10^{-17} at 100 Hz and less than 10^{-18} at 500 Hz. We also identify a particularly interesting type of transition in between the LVK and LISA bands and show how multi-band observations can constrain this further. Finally, we discuss what these current and forecasted constraints imply for the underlying dark energy theories.

CONTENTS

Open access

12

| | |
|--|----|
| I. Introduction | 1 |
| II. From theory to templates | 2 |
| A. Dark energy and $c_{\text{GW}} \neq c$ | 2 |
| B. The reach of a theory and frequency-dependent c_{GW} | 3 |
| C. Templates for c_{GW} | 4 |
| III. The gravitational wave signal | 5 |
| A. Waveform stretching or squeezing | 5 |
| B. Arrival times | 6 |
| C. Intrinsic source effects | 6 |
| IV. Probing c_{GW} in the LVK band | 6 |
| A. Including waveform stretching/squeezing in the gravitational wave signal | 7 |
| B. Parameterizing $\delta c_{\text{GW}}(f)$ | 7 |
| C. Approximate measurement of observable c_{GW} deviation | 7 |
| D. Bayesian parameter estimation constraints of c_{GW} using GW170817 | 8 |
| V. Probing c_{GW} in the LISA band | 9 |
| VI. Probing c_{GW} with joint LVK/LISA observations | 10 |
| VII. Conclusions | 11 |
| Acknowledgments | 12 |
| Data availability | 12 |

| | |
|---|----|
| A. c_{GW} in Horndeski gravity | 12 |
| B. More c_{GW} templates | 13 |
| C. Intrinsic source evolution with non-constant c_{GW} | 13 |
| D. Constraints using only LVK or ET observations | 15 |
| References | 15 |

I. INTRODUCTION

One of the most fundamental observables in testing our understanding of gravity is the speed with which gravity propagates. In a Lorentz-invariant solution, gravitational waves will propagate at the speed of light, but this need not be the case if Lorentz invariance is spontaneously broken, as it is in our Universe. Here, just as for any other waves, the speed of gravitational waves c_{GW} depends on the medium they are propagating through. Measuring c_{GW} therefore lets us probe the nature of this medium. With dark energy accounting for close to 70% of the energy budget of our current Universe [1], constraining c_{GW} provides an especially powerful tool in hunting for new degrees of freedom potentially associated with dark energy or a modified theory of gravity. Such new degrees of freedom, which non-trivially affect the background evolution and hence the universal ‘medium’, are a generic consequence of departures from modelling dark energy as a cosmological constant Λ . Tight constraints found on some such theories [2–5] – also see earlier related work [6–16] – following the joint observations of GW170817 and GRB 170817A [17–21] neatly illustrate this point.

Current constraints on the speed of gravitational waves, c_{GW} , strongly depend on the frequency range in question and

* Corresponding author: ian.harry@port.ac.uk

† Corresponding author: johannes.noller@port.ac.uk

are conveniently expressed in terms of the parameter

$$\alpha_T \equiv (c_{\text{GW}}^2 - c^2)/c^2, \quad (1)$$

where c is the speed of light. Note that α_T therefore is a measure of the ‘tensor speed excess’, i.e. it is positive for $c_{\text{GW}} > c$ and negative when $c_{\text{GW}} < c$. We will remain agnostic here and will not assume anything about the sign of α_T in what follows¹. Constraints from the cosmic microwave background and large scale structure (see [24–49] and references therein), corresponding to frequencies $f \sim 10^{-18} - 10^{-14}$ Hz, require $|\alpha_T| \lesssim \mathcal{O}(1)$. Binary pulsars, in particular the Hulse-Taylor binary, impose $|\alpha_T| \lesssim \mathcal{O}(10^{-2})$ for frequencies $f \sim 10^{-4}$ Hz [14]. Gravitational wave observations of the afore-mentioned GW170817 event then place an extremely tight bound of $|\alpha_T| \lesssim \mathcal{O}(10^{-15})$ for frequencies $f \sim 10^1 - 10^3$ Hz [17–21], while the presence of high energy cosmic rays (and inferred absence of gravitational Cherenkov radiation) leads to a $\alpha_T \gtrsim -\mathcal{O}(10^{-15})$ bound at energies of $\sim 10^{10}$ GeV [50], i.e. for very high frequencies $f \sim 10^{34}$ Hz. Note that the last bound *does* depend on the sign of α_T . Finally, several forecasted bounds exist for future LISA observations [51, 52]. Since these are particularly relevant in the context of this paper, we will discuss them in more detail in section V. The frequency-dependence of the bounds on α_T is particularly important, since the theoretical predictions for this parameter are also frequency-dependent. More specifically, for large classes of dark-energy related models that yield a significantly non-zero α_T on cosmological scales, i.e. at very low frequencies, one naturally expects a transition back towards $\alpha_T = 0$ close to or somewhat below 10^2 Hz [53]. This means that the tight GW170817 constraint on α_T is perfectly consistent with models that yield a detectable, non-zero α_T at lower frequencies.

Current ground-based observatories, Advanced LIGO [54], Advanced Virgo [55] and KAGRA [56] have sensitivity between approximately 20 Hz and ~ 2000 Hz. In the coming years, these observatories will continue to run a series of increasingly sensitive observing runs, with lower frequency sensitivity reaching no lower than 10 Hz [57]. It is expected that these runs will yield numerous observations of binary neutron star mergers, and hopefully numerous multimessenger observations [57], with which powerful tests of the speed of gravity can be performed. However, to perform tests outside of this frequency range we must wait for the next generation of gravitational-wave observatories, expected to become operational in the 2030s. The third generation of ground-based observatories, Einstein Telescope [58] and Cosmic Explorer [59], will increase overall sensitivity, and increase the range of sensitive frequencies, covering from ~ 1 Hz up to $\sim 10^4$ Hz. Perhaps of most interest in this context though are the proposed space-based observatories, LISA [60] and TianQin [61], which will cover a range of frequencies inaccessible from the ground, covering $\sim 10^{-4}$ Hz to $\sim 10^{-1}$ Hz.

In this paper we investigate how observations from the LIGO/Virgo/KAGRA observatories (henceforth LVK), and GW170817 in particular, can be leveraged to provide additional constraints on a frequency-dependent transition of c_{GW} , extending existing constraints that assume a frequency-independent c_{GW} . We also explore how one can use lower frequency measurements of gravitational waves in the LISA band to test for the existence and nature of such a transition and how one might be able to combine information from both space-based and ground-based observation bands to provide further constraints.

The paper is structured as follows. In section II we discuss in what sense the frequency-dependence of c_{GW} is a generic phenomenon in models that do lead to a non-zero α_T on cosmological scales. As a key outcome of this discussion, we introduce and motivate templates to capture this frequency dependence. In section III we investigate what the imprint of a frequency-dependent c_{GW} is on the gravitational wave signal observed, highlighting the resulting stretching and squeezing of the waveform as the main associated observable. In the following sections we then compute constraints and forecasts on the frequency-dependence of c_{GW} : In section IV we present constraints computed for the LVK band, that extend existing bounds on a constant and hence frequency-independent c_{GW} . In section V we present analogous forecasts for the LISA band, and in section VI we discuss how joint observations in both bands will allow us to place highly precise constraints on c_{GW} over the whole range of relevant frequency and energy scales. We conclude and summarise our findings in VII and collect additional details in the appendices.

II. FROM THEORY TO TEMPLATES

In this section we will illustrate how a non-luminal c_{GW} can arise in theories of dark energy (II A), why this generically leads to a c_{GW} that is frequency-dependent, where (if indeed present) one would expect this to be especially pronounced close to the frequencies observed by present (LVK) and near-future (LISA/TianQin/Einstein Telescope/Cosmic Explorer) detectors (II B), and how one can use this information to build theoretically well-motivated templates to be used in constraining and searching for frequency-dependent c_{GW} (II C).

A. Dark energy and $c_{\text{GW}} \neq c$

Since GR is the single consistent theory of a massless spin-2 field, testing for (potentially dark energy-related) deviations away from it generically amounts to probing the presence of new gravitational degrees of freedom. Scalar-tensor theories are a minimal deviation from GR in this sense, as they only introduce a single additional degree of freedom. Accordingly, Horndeski gravity [62, 63]², the most general Lorentz-invariant scalar-tensor action that gives rise to second order

¹ It is useful to recall that for a spontaneously Lorentz-breaking solution, $c_{\text{GW}} \leq c$ need not be imposed by causality requirements – in fact the opposite can be the case, see e.g. [22, 23] and references therein.

² For the equivalence between the formulations of [62] and [63], see [64].

equations of motion, has recently been the main workhorse in testing for deviations from GR. In appendix A we will summarise the key relevant results for the complete Horndeski theory, but here we will illustrate the salient points with the following example scalar-tensor theory³

$$\mathcal{L} = \frac{M_{\text{Pl}}^2}{2} R - \frac{1}{2} \nabla_\mu \phi \nabla^\mu \phi + \frac{M_{\text{Pl}}^2}{\Lambda^3} g(\phi) G_{\mu\nu} \nabla^\mu \nabla^\nu \phi. \quad (2)$$

The first two terms are the standard kinetic interactions for the massless tensor $g_{\mu\nu}$ and the scalar ϕ , respectively, while the last term is a higher-order interaction involving both the scalar and tensor. $G_{\mu\nu}$ is the Einstein tensor and $g(\phi)$ is a dimensionless function of ϕ/M_{Pl} . There are two key mass scales: the Planck mass M_{Pl} , and the scale Λ associated with second derivatives of the scalar. In cosmology these are linked to the value of the Hubble constant today, H_0 , and are conventionally taken to satisfy $\Lambda^3 = M_{\text{Pl}} H_0^2$. This choice ensures that all interactions can give $\mathcal{O}(1)$ contributions to the (cosmological) background evolution, so is phenomenologically motivated in order to allow the scalar ϕ to act as dark energy.

We can now work out the speed of gravitational waves c_{GW} for the theory (2). In a scalar-tensor theory as we are considering here, gravitational waves propagate through a ‘medium’ provided by the presence of the scalar ϕ . The interactions of ϕ with $g_{\mu\nu}$ encoded in (2) can affect the refractive index of this medium and hence c_{GW} . More specifically, we find

$$\alpha_T = \frac{2(\nabla\bar{\phi})^2 g'(\bar{\phi})}{M_{\text{Pl}} \Lambda^3 - (\nabla\bar{\phi})^2 g'(\bar{\phi})}, \quad (3)$$

where a prime denotes a derivative with respect to the argument of the function (we recall this is ϕ/M_{Pl} for g and so both g and g' are dimensionless) and $\bar{\phi}$ is the background solution for the scalar. This makes it clear that for a Lorentz-invariant background solution with $\bar{\phi} = 0$ we obtain $\alpha_T = 0$ and hence gravitational waves travel at the speed of light there, as expected. However, when considering the cosmological background solution $\bar{\phi} = \bar{\phi}(t)$ of interest here, this time-dependent scalar evolution spontaneously breaks Lorentz invariance and provides a non-trivial medium for gravitational waves to travel through. In this case, α_T will generically be non-zero and we obtain the following dispersion relation

$$\omega^2 = c_{\text{GW}}^2(t) k^2, \quad (4)$$

where $c_{\text{GW}}^2 = (1 + \alpha_T) c^2$ as above. We emphasise that this means α_T is generically *time-dependent*, but (so far) *frequency-independent* – we will see how frequency-dependence enters below. Regarding the time-dependence, note that the characteristic timescale for this in theories of dark energy is a Hubble time ($1/H_0 \sim 10^{10}$ years). Compared to the characteristic travel time for the signals seen by

gravitational wave detectors this is approx. the same order of magnitude for a source at a distance of \sim Gpc (travel time $\sim 3 \times 10^9$ years) and about two orders of magnitude larger for closer sources (the travel time is $\sim 10^8$ years for a source at 40 Mpc), assuming the signal travels at close to the speed of light. While taking into account this time-dependence can therefore have a noticeable effect for far-away sources, e.g. modulating some of the relevant observables such as arrival times, this will not change the qualitative, order-of-magnitude constraints we are focusing on here. We will therefore ignore any time-dependence here and leave an exploration of this effect to future work⁴.

B. The reach of a theory and frequency-dependent c_{GW}

Let us return to the example theory (2). The higher-order interactions encoded in the final term mean this theory is predictive at most up to the energy scale Λ and cannot resolve energy scales close to or larger than this – see e.g. [69–71] for reviews of the underlying field theoretic reasoning. This is precisely analogous to what happens in GR, which also encodes higher-order interactions within the Einstein-Hilbert term and where predictivity is lost as one approaches the corresponding energy scale there, namely the Planck scale. For cosmologically motivated models, where the scalar ϕ is linked to dark energy, we recall that $\Lambda^3 = M_{\text{Pl}} H_0^2$. Expressed as a frequency this amounts to

$$\Lambda \sim 260 \text{ Hz}. \quad (5)$$

This is the largest possible energy/frequency scale, a so-called cutoff, where (2) stops being applicable. Making predictions around or above this scale then requires knowledge of a more complete high energy theory, a UV completion, that extends the regime of validity of this theory beyond the frequency/energy scale Λ . In the absence of knowledge about such a UV completion, i.e. in the field’s present situation, we simply do not know how to relate a measurement at energies $\gtrsim \Lambda$ to a theory such as (2). Note that this conclusion does not rely on the specific form of (2) and affects all sectors of the theory involving ϕ interactions⁵. It is worth emphasizing that Λ is the *largest* possible scale up to which such a theory can be predictive. Where precisely this threshold is depends on the specific nature of the UV completion. Compare this

³ We emphasise that we merely use (2) as an example to illustrate generic α_T features in scalar-tensor theories. While they will not be important here, we refer the reader curious about some of the interesting stability/screening/positivity properties of (2) to [64–68] and references therein.

⁴ Note that, while dark energy only becomes a major driver of the cosmological evolution from $z \sim \mathcal{O}(1)$ onwards, it only takes light approx. twice as much time to travel to us from redshift 1 vs. from redshift 1000, so this difference is immaterial to what we are doing here.

⁵ More specifically, it is precisely the interactions that affect α_T which depend on Λ and hence limit the applicability of the theory to energy scales below Λ . In other words, if ϕ interactions in a Horndeski theory contribute to the dark energy evolution today and affect α_T on cosmological scales, this naturally leads to a cutoff (5). So this conclusion does indeed not rely on the specific example (2). Some (but not all) well-known dark energy theories that do not affect α_T can have a much larger cutoff, e.g. quintessence [72–75] or k-essence [76–79] theories.

with the Fermi theory for weak interactions, where the naive cutoff scale is $\sim \text{TeV}$, yet new physics associated with a UV completion already enters an order of magnitude below at the scale of the W-boson at $\sim 80 \text{ GeV}$. The LISA and lower end of the LVK bands (as well as intermediate bands) are therefore particularly well-motivated regions to look for the onset of new physics associated with UV completions of dark energy theories.

How is the above discussion of regimes of validity for scalar-tensor theories relevant to the main observable we are considering in this paper, c_{GW} ? This is discussed in detail in [53] and we here summarise the essential results relevant for this paper. When deriving (3) and (4) we were implicitly working on cosmological scales, firmly within the regime of validity of (2). However, as one approaches the cutoff of the theory $\lesssim \Lambda$, the existence of a UV completion will manifest itself by additional interactions (highly suppressed on cosmological scales) becoming important. Precisely what these interactions are is determined by the (unknown) UV completion, but we can infer some types of candidate additional interactions from investigating radiative corrections to generic Horndeski theories [36, 80–91]. The example set of such interactions focused on in [53] is

$$\mathcal{L}^{(n)} = M_{\text{Pl}}^2 G_{\mu\nu} \frac{\square^n}{M^{2n+4}} (\nabla^\mu \phi \nabla^\nu \phi), \quad (6)$$

where $M \lesssim \Lambda$ is the scale associated with these UV-induced new operators and $n \geq 2$. Of particular relevance for our context is the (representative and generic) higher-derivative nature of these interactions. Including these interactions modifies the dispersion relation (4) and one now finds [53]

$$\omega^2 \sim c_{\text{GW}}^2(0)k^2 + \sum_{n \geq 2} \frac{c_n \Lambda^6}{3M^{2n+4}} (c^2 k^2 - \omega^2)^{n-1} (\omega^2 + \mathcal{O}(k^2)), \quad (7)$$

where ω is the angular frequency, k the wavenumber, the c_n are some order one coefficients (whose precise value is not important here) and we have ignored suppressed H -dependent corrections, since $H^2/\omega^2 \ll 1$ for the frequencies relevant here. Here we explicitly write c_{GW} as a function of k and hence denote the asymptotic value of c_{GW} for low energies/frequencies, i.e. effectively its cosmological value derived in (3), by $c_{\text{GW}}(0)$ – see [53] for details on the derivation of the full dispersion relation for this example as well as other related examples. Crucially, (7) asymptotes to the cosmological $c_{\text{GW}} = c_{\text{GW}}(0)$ for small k (low frequencies) and asymptotes to luminal $c_{\text{GW}} = c$ for large k (high frequencies), where the $(c^2 k^2 - \omega^2)^{n-1}$ drives this large k approach to luminosity. Here it is important to emphasise the point made by [53] that asymptoting to $c_{\text{GW}} = c$ at high energies, as is entailed by (7), is a generic consequence of any UV completion as long as Lorentz invariance is restored at scales $\gtrsim M$. So this feature should certainly not be seen as an accident of the example interactions shown here.

Finally, it is instructive to consider the asymptotic scaling of c_{GW} with k deriving from (7). We focus on a single n interaction in (6) and denote the values of k and f corresponding to

the transition scale $M \lesssim \Lambda$ by k_* and f_* , respectively, in what follows. Doing so, we find

$$\begin{aligned} k \ll k_* : & \quad c_{\text{GW}} - c_{\text{GW}}(0) \propto k^{2n-2}, \\ k \gg k_* : & \quad c - c_{\text{GW}} \propto k^{-2}. \end{aligned} \quad (8)$$

We see that there is a clean power law scaling in both limits, where the relevant power for small k depends on the precise interaction term present, while there is a universal $1/k^2$ approach to luminal c_{GW} for large k . With an eye on constructing templates below, it is very important to separate what is a generic feature any template should recover vs. what is an accident of the example chosen. At scales below the transition scale k_* , a UV completion will indeed generically give rise to higher-derivative interactions such as (6). In the dispersion relation these will manifest themselves as higher powers of k suppressed by the scale M , so generically one does indeed expect that a power law scaling is an excellent approximation for the low energy approach into the c_{GW} transition. However, once reaching energy scales $\sim M$ (or equivalently k_*) no firm prediction of the transition behaviour can be made without the (unknown) UV completion. In particular, the transition can in principle happen arbitrarily quickly and need not even follow a power law. So the universal $1/k^2$ scaling found for the simple example above should *not* be hard-coded into any template⁶. Furthermore, when going beyond the simple example above and considering a generic situation where all c_n can be non-zero, a different large k scaling can be obtained for a given $c_{\text{GW}}(0)$ by carefully tuning the c_n . Judging whether such a tuning is natural again requires detailed knowledge of the UV completion, but this already provides further reason why no fixed power-law dependence for large k should be hard-coded into any template⁷.

C. Templates for c_{GW}

In the sections below we will use current/forecasted observational data from LVK and LISA bands to place constraints on the frequency-dependence of c_{GW} . Doing so generically requires a template for the waveform and, in particular, for c_{GW} itself. Given the above considerations and plethora of potentially contributing interactions, the precise form of $c_{\text{GW}}(f)$ in principle depends on a large number of parameters. This includes the c_n in (7), and crucially parameters associated to the unknown UV completion that generically becomes important in or close to the LVK/LISA bands for dark energy theories leading to a non-luminal c_{GW} at very low frequencies, i.e. for cosmology.

⁶ As we shall see in more detail later, transitions that do have a ‘slow’ $1/k^2$ scaling at high energies are severely constrained by LVK measurements such as GW170817 even when the analogue of f_* (and hence k_*) are firmly within the LISA band. But while this is of course an interesting finding for transitions with this scaling in its own right, it should not be mistaken for a generic conclusion.

⁷ We thank Scott Melville for related discussions.

We would therefore like to work with a template for c_{GW} that, while simplifying the parametric dependence and making an analysis practical, still captures the salient features of this frequency-dependence. As discussed above, such a template ought to asymptote to a luminal c_{GW} at large frequencies (to enable consistency with LVK bounds), asymptote to a constant $c_{\text{GW}}(0)$ at small frequencies (consistent with (3)), while also allowing different scalings with k throughout the transition. A minimal template will depend on at least three parameters

- A speed $c_{\text{GW}}(0)$, which corresponds to the asymptotic speed of gravitational waves at low frequencies. Effectively this is the cosmological c_{GW} that can differ significantly from c .
- A frequency scale f_* , denoting the ‘central frequency’ of the transition from $c_{\text{GW}}(0)$ to c . In terms of the underlying physics this is set by the scale where new physics associated with the UV completion becomes important, e.g. M in (6).
- A parameter σ , which controls how quickly the transition takes place. This is effectively a measure of the nature of the new interactions present due to the UV completion.

Note that there can in principle be many more parameters controlling interactions that determine how quickly the transition takes place, so introducing a single parameter for this should be seen as a lowest order approximation.

Using the parameters listed above, we can build the following useful hyperbolic fitting function

$$\Theta_{\pm}(f, \sigma, f_*) \equiv \frac{1}{2} \pm \frac{1}{2} \tanh[\sigma \cdot \log(f/f_*)], \quad (9)$$

where Θ_+ transitions between 0 and 1 around f_* , while Θ_- transitions from 1 to 0 around the same frequency. σ controls how quickly this transition takes place, as advertised. With this function we can now build a straightforward template for c_{GW} as a function of frequency f , that captures the essential features outlined above

$$c_{\text{GW}}(f, \sigma, f_*) = c_{\text{GW}}^{(0)} + (c - c_{\text{GW}}^{(0)})\Theta_+. \quad (10)$$

This behaviour is illustrated in Figure 1.

It is again instructive to consider asymptotic scalings with k . From (10) we find

$$\begin{aligned} k \ll k_* : & \quad c_{\text{GW}} - c_{\text{GW}}(0) \propto k^{2\sigma}, \\ k \gg k_* : & \quad c - c_{\text{GW}} \propto k^{-2\sigma}. \end{aligned} \quad (11)$$

This clearly shows that the steepness parameter σ directly controls the power law scaling in both asymptotic limits, allowing us to mimic different UV-completion-induced scalings at high energies. Due to the simplicity of the template, the single parameter σ controls both asymptotes and hence we have symmetric $k^{2\sigma}$ and $k^{-2\sigma}$ scalings for this template. There is no fundamental reason why the transition ought to be symmetric in this way and it is straightforward to refine the template

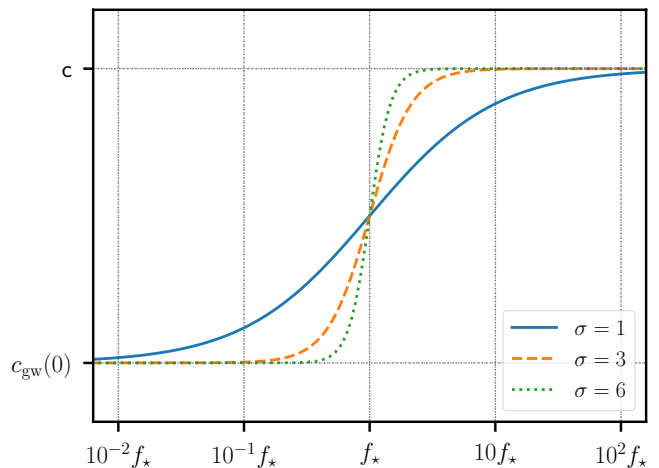


FIG. 1. The speed of gravitational waves, c_{GW} , as a function of frequency f for the templates discussed in section II. The different curves correspond to different choices of the ‘steepness’ parameter σ that also controls the asymptotic power law scalings of the c_{GW} – see (11). c_{GW} neatly interpolates between $c_{\text{GW}}(0)$, the speed of GWs on cosmological scales, and the speed of light c at large frequencies. f_* physically gets set by the scale $M \lesssim \Lambda$ that marks the onset of the UV completion for the dark energy theory in question, cf. (6).

to include asymmetric transitions upon introducing an additional parameter – see appendix B⁸. However, for the constraint analysis in the following sections we will work with the minimal template (10) and leave a more detailed analysis of more refined templates including additional corrections for future work.

III. THE GRAVITATIONAL WAVE SIGNAL

Before proceeding to probing c_{GW} using current and forecasted data, we will find it useful to understand some key features of the GW signal itself.

A. Waveform stretching or squeezing

If any detectable form of frequency-dependence (we will be more quantitative below) takes place within the observable LVK and/or LISA bands, where the source is tens to thousands of megaparsecs away from the detectors, the leading-order effect of a frequency-dependent c_{GW} will be that the observed signal is stretched (for negative α_T) or squeezed (for positive α_T) as the travel time varies with frequency.

⁸ We also emphasise that the most highly UV sensitive (and hence least robust) features of the transition, e.g. the precise functional form around f_* in (7) (which are generically different for the small and large frequency asymptote) are not reproduced by the template by design.

The travel time of a signal between a source and an observer on the Earth can be expressed as

$$t = \frac{D_L}{c_{\text{GW}}(f)} \equiv \frac{D_L}{c(1 - \delta c_{\text{GW}}(f))} \approx \frac{D_L}{c} + \frac{D_L}{c} \delta c_{\text{GW}}(f), \quad (12)$$

where D_L is the luminosity distance to the source. We define here $\delta c_{\text{GW}}(f) \equiv 1 - c_{\text{GW}}(f)/c$, which is the fractional variation in the gravitational-wave speed from c . This is related to α_T according to $\alpha_T = -2\delta c_{\text{GW}} + (\delta c_{\text{GW}})^2$, the latter term being negligible in the cases that we will consider. $\frac{D_L}{c} \delta c_{\text{GW}}(f)$ then denotes the frequency dependent time delay that is incurred if c_{GW} is less than c . As the frequency of radiation emitted by the source increases, waves emitted at different times (and hence different frequencies) will have a different associated $\delta c_{\text{GW}}(f)$ (and hence travel times). This is what leads to the stretching/squeezing of the observed signal, where importantly the distance to the source affects how pronounced this effect is. We note that this squeezing and stretching affect is the same as the frequency-domain dephasing introduced in [92], albeit expressed in a different formalism. In the case of a large distortion in the observed waveform, this can lead to effects analogous to the ‘inverse chirping’ of scalar waves in scalar-tensor theories [93, 94]. For distances of 100Mpc a value of only $\delta c_{\text{GW}}(f) = 1 \times 10^{-16}$ is required to add a shift of 1s to a signal. While 1 second may seem like a small amount, shifting a signal by 1 second in the tens of seconds it takes a signal to move through the LVK observing band is a significant shift, as we will explore in more detail in later sections.

B. Arrival times

A second case of interest is when there is no detectable frequency-dependence in the LVK or LISA bands themselves, yet there is a sharp transition in between the two bands. In that case systems that are first observable in LISA and then enter the LVK band are an excellent probe of the transition. The primary signature here is not in the form of the signal itself, but instead even a small δc_{GW} will result in an ‘arrival time’ of the signal in the LVK band significantly different from what would be predicted from LISA observations of the signal itself. The idea of multi-band observations—using information from both LISA and the LVK band to measure the properties of compact binary mergers—was first demonstrated in [95]. In that work it was predicted that LISA observations could measure the arrival time of the signal in the LVK band to an accuracy of tens of seconds. This finding was later supported by more detailed followup work [96, 97]. However, in an independent study [98], a more pessimistic prediction was provided. There it is found that for stellar-mass black systems, like GW150914, one can predict the arrival time in the LVK band with a precision of \sim hours from observations in the LISA band. This discrepancy has not yet been resolved in the literature⁹. Nevertheless, even an uncertainty on the arrival

⁹ We thank the authors of [97, 99] for related discussions.

time of the signal in the LVK band constrained to hours can in principle be used to place very strong constraints on δc_{GW} in the case of multi-band observations, as we explore in section VI.

C. Intrinsic source effects

We will explore the effect of the waveform stretching/squeezing and arrival time further in the following sections, but first we will briefly state that the emission of gravitational waves is affected when a non-trivial c_{GW} is present even when one is very near to the source. The full derivation can be found in appendix C, but we show that the intrinsic evolution of the source, in terms of the angular frequency (ω), is changed in the presence of a non-constant c_{GW} according to

$$\dot{\omega}(t) = \left(\frac{G_{\text{GW}}c}{G_N c_{\text{GW}}} \right) \frac{3456^{1/3}}{5} \left(\frac{G_N M_c}{c^3} \right)^{5/3} \omega^{11/3}. \quad (13)$$

Here G_{GW} is the effective gravitational ‘constant’ G seen by tensor perturbations in the metric and G_N is the ‘standard’ gravitational constant as e.g. entering the Poisson equation or Kepler’s laws¹⁰. This is the standard general relativity solution, computed to leading order (“0 Post-Newtonian order”), with an additional term containing c_{GW} and G_{GW} . However, as shown in appendix C, this term/correction will be negligible in comparison to the arrival time delays (in the region we are exploring), so we will neglect this effect in what follows.

IV. PROBING c_{GW} IN THE LVK BAND

The joint observation of GW170817 and GRB 170817A allowed for a simple, but very powerful, test of the speed of gravity. The peak of gravitational-wave emission and the gamma-ray burst arrived at the Earth within seconds of each other. If one assumes that these were emitted from the source at roughly the same time, then any deviation between their arrival times at the Earth would be due to differences in the speed of the two messengers. In the absence of any observable delay, a very strong bound on c_{GW} can be placed. Indeed, this observation constrained δc_{GW} in the 10 - 1000Hz frequency band to $\lesssim 3 \times 10^{-15}$ [20].

This limit was placed assuming a *constant* c_{GW} . In the scalar-tensor theories we consider here we assume that δc_{GW} is allowed to be nonzero, but it must be asymptoting to 0 in the > 10 Hz frequency band in which GW170817 was observed by LIGO and Virgo. We will demonstrate that a

¹⁰ In other words, G_N is the gravitational constant relevant for the interaction between (test) masses, so e.g. for the computation of planetary orbits or torsion balance tests, while (in the context of the Horndeski theories considered here) gravitational waves feel a different effective gravitational constant G_{GW} due to the presence of the extra scalar degree of freedom. For Horndeski theories these satisfy the relationship $G_N/G_{\text{GW}} = c_{\text{GW}}^2/c^2$ [14] – see appendix C for details.

much tighter constraint on δc_{GW} across the LVK sensitive band can be placed whenever there is a frequency-dependent c_{GW} . To do this we will first formulate how we will model the gravitational-wave signal that ground-based observatories would see assuming a variable c_{GW} , we will then define how we will model our specific example, and then use these models to identify what range of c_{GW} is consistent with the data observed around GW170817.

A. Including waveform stretching/squeezing in the gravitational wave signal

We first need to define how we will apply a frequency-dependent δc_{GW} to the waveforms that we will be using. As discussed in section III C, we neglect any intrinsic source evolution effects. However, the variable travel time delay as the waveform evolves from 10Hz towards 1000Hz and merger is not negligible, and we must incorporate this effect into our waveform models.

To do this we begin by using the ‘‘TaylorF2’’ post-Newtonian waveform [100] as implemented in `lalsuite` [101], and apply a frequency-dependent time shift to it. We first identify time before merger (τ) as a function of frequency using the leading order general relativity approximation

$$f = \left(\frac{256}{5c^3} M_c^{5/3} \pi^{8/3} \tau \right)^{-3/8}. \quad (14)$$

We then identify the time delay as a function of frequency according to

$$\delta\tau(f) = \frac{D_L}{c} \delta c_{\text{GW}}(f). \quad (15)$$

From these two expressions we can get $\delta\tau(\tau)$ —the arrival time delay as a function of time before merger—which can be used to produce the timeshifted waveform we might expect to observe under these assumptions. We apply the frequency dependent time shift by Fourier transforming the frequency-domain waveform into the time-domain, applying the time shift to all sample points, and interpolating the waveform back to an equally spaced timeseries for use in analysis.

We note that our interpolation technique is computationally expensive. The technique of adding this squeezing and stretching in terms of phase offset in the frequency domain [92] is more efficient, but would need to be generalized from the power-law case considered there (although we do use a power-law approximation in this section, we use the form of equation 10 in later sections). We also only consider the dominant mode of gravitational-wave emission in our studies, we refer the reader to [102] for a discussion on how higher-order modes could be included.

B. Parameterizing $\delta c_{\text{GW}}(f)$

We next need a functional form of $\delta c_{\text{GW}}(f)$. We use the formalism we discussed in section II C in the limit where

$\delta c_{\text{GW}}(f)$ is asymptoting to 0, i.e. in what we previously called the $k \gg k_*$ limit. We model this asymptotic behaviour with two parameters— $\delta c_{\text{GW}}(f_{\text{ref}})$ and σ —according to

$$\delta c_{\text{GW}}(f) = \delta c_{\text{GW}}(f_{\text{ref}}) \times \frac{f_{\text{ref}}^{2\sigma}}{f^{2\sigma}}. \quad (16)$$

Here e.g. $\delta c_{\text{GW}}(30)$ corresponds to the value of δc_{GW} at 30 Hz, and we assume that δc_{GW} is approaching zero over the band of observation following a power law with slope 2σ . f_{ref} is some reference frequency, which we stress is distinct from f_* . Note that this emergent power law behaviour neatly links up with power-law parametrisations for (modifications of) the dispersion relation previously employed in the literature [52, 92, 103]. However, it is worth emphasizing that in our context this behaviour only emerges asymptotically and it will eventually be important to keep track of the full functional form of (10) when inferring constraints on $\delta c_{\text{GW}}(f)$ throughout the entire range of frequencies considered here. We will do so in the following sections.

C. Approximate measurement of observable c_{GW} deviation

We then want to quantify if such a deviation in the waveform is observable with respect to a waveform where always $c_{\text{GW}} = c$. A way to approximate what values of $\delta c_{\text{GW}}(f_{\text{ref}})$ and σ are required to produce a distinguishable effect is to use the ‘‘distinguishability criteria’’ from [104]. This states that two waveforms are considered to be distinguishable if, after subtracting one from the other, the residual has a signal-to-noise ratio that is larger than one. That is if

$$\langle h_2 - h_1 | h_2 - h_1 \rangle \geq 1 \quad (17)$$

then two waveforms could be distinguished from each other. This uses the definition of the noise-weighted inner product between two waveforms h_1 and h_2 , which is commonly used in gravitational-wave data analysis

$$\langle h_1 | h_2 \rangle = 4\Re \int_0^\infty \frac{h_1^*(f) h_2(f)}{S_n(f)} df. \quad (18)$$

Then, to find the level of deviation which is observable, we first choose a fiducial physical system and generate the waveform assuming GR. We then generate the same waveform, but assuming some parameterized deviation from GR and measure the ‘‘distinguishability criterion’’. We then vary the values of the GR-deviation parameters until we get a value of 1. We note that this measure can provide overly optimistic predictions in the case where there are correlations between parameters, for example it might be possible to change other physical parameters to mimic the waveform stretching/squeezing. We will check the validity of this approximation in the following subsection.

In the top panel of Figure 2, we demonstrate this for a signal with the same masses and signal-to-noise ratio as GW170817, and using the Advanced LIGO noise curve. This allows us to predict that such a signal would allow us to constrain δc_{GW}

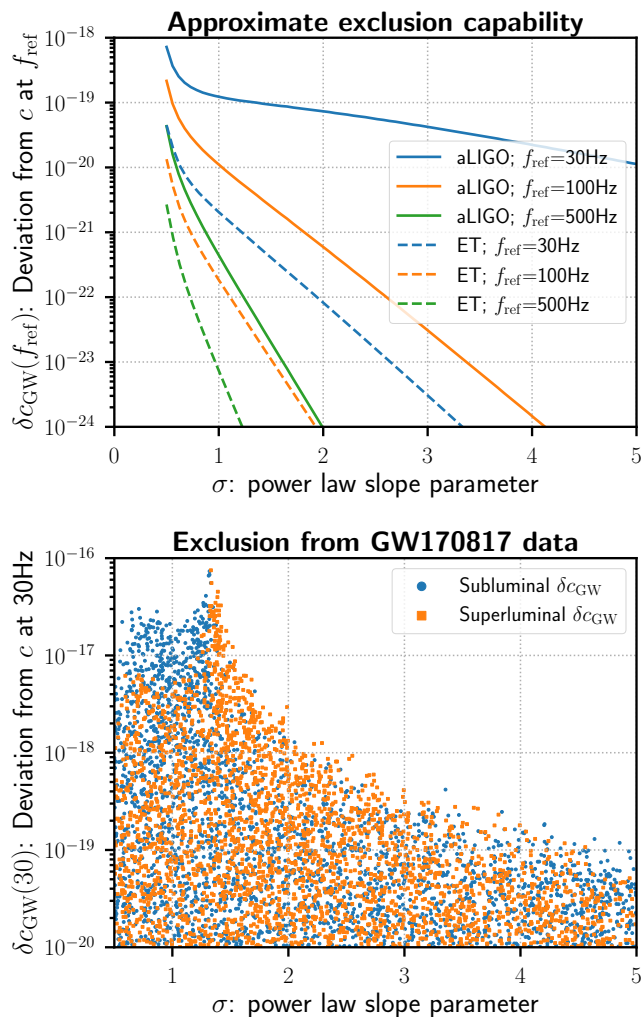


FIG. 2. (Top) A prediction of how well we would be able to constrain δc_{GW} at 30Hz, 100Hz and 500Hz as a function of the power law slope parameter σ . This power law models how quickly $\delta c_{\text{GW}}(f)$ asymptotes to 0 as the frequency increases. This prediction assumes a signal with the same masses ($1.36M_{\odot}$ for both bodies) as GW170817, and the same signal-to-noise ratio (32.4). The Advanced LIGO noise curve and the Einstein Telescope predicted noise curve [101] are used while computing these predictions. (Bottom) Bayesian inference exclusion posterior points, projected down to σ and $\delta c_{\text{GW}}(30)$. An animated version of this panel can be found at [THIS LINK](#)

at 30Hz to be no larger than $\sim 10^{-19}$, for a slope with power law $\sigma = 1$. For larger values of n the exclusion quickly becomes much tighter. We also predict the exclusion of δc_{GW} at 100Hz and 500Hz. Exclusions at these frequencies are considerably tighter, as would be expected when we model δc_{GW} as asymptoting to 1. Finally, we predict the exclusion that would be possible if GW170817 were observed with the future Einstein Telescope observatory, these exclusions are around two orders of magnitude tighter at $\sigma = 1$ and decay considerably quicker, reflecting the improved sensitivity of Einstein Telescope at lower frequencies. This figure is generated assuming

a subluminal c_{GW} , however we find that the results are identical to within numerical precision when using a superluminal c_{GW} ¹¹.

For full reproducibility of this, and other figures in this work, the code used to produce this figure can be found by [clicking on this link](#).

D. Bayesian parameter estimation constraints of c_{GW} using GW170817

We next consider what constraints can be placed using the recorded strain data around the GW170817 observation when a frequency-varying c_{GW} is assumed. This will allow us to verify the predicted curve in Figure 2 and check to see if there are correlations between the parameters parameterizing δc_{GW} and other physical parameters of the system. We use Bayesian inference to place bounds on the σ and $\delta c_{\text{GW}}(30)$ parameters. We take the publicly released data from GWOSC from around GW170817 [105] and follow closely the analysis described in [106]. We take the known sky location from the optical counterpart to GW170817 [21] and assume a luminosity distance of 40Mpc [107] when applying the frequency-dependent time shift. We do not consider spins in the analysis as neutron star spins are expected to be small [108], which allows us to reduce computational cost and we also do not include tidal terms in the waveform.

We choose a prior on σ that is uniformly distributed between 0.5 and 5, and a uniform in log prior on $\delta c_{\text{GW}}(30)$ between 1×10^{-13} and 1×10^{-20} . Other prior ranges match those of [106]. We use the emcee parallel tempered sampler [109] within PyCBC inference [110] to generate results. We run the analysis twice, once allowing for only subluminal values of c_{GW} and once allowing for only superluminal values of c_{GW} . The results are then combined for visualization. For full reproducibility, the configuration files and code versions can be found in our data release page.

We can see the results of the Bayesian analysis in the bottom panel of Figure 2. We observe that the exclusion plots strongly depend on the frequency dependence of c_{GW} , i.e., on the power law slope σ in Equation 11. The vast majority of samples we obtain have a δc_{GW} at 30Hz smaller than $1 \times 10^{-16.5}$, although there is one curious spike where $\sigma \sim 1.5$, where a shift in the masses of the source, coupled with this particular frequency-dependent time shift, seems to reproduce the GW170817 waveform well. This occurs for both superluminal and subluminal c_{GW} , although the shifted source masses differ in the two cases. We also provide an animated version of this plot, where we show how the constraints improve as a function of frequency. We find that all samples have δc_{GW} smaller than 1×10^{-17} at 100Hz, and all samples are smaller than 1×10^{-18} at 500Hz. We can also compare the

¹¹ In the next section we do find slightly different behaviour between subluminal and superluminal c_{GW} . This is because a partial degeneracy between source masses and the deviation parameters becomes important, and at some points we see divergence between the two cases.

results between the two panels of Figure 2 to validate the accuracy of the distinguishability criterion used in the top panel. While we do notice that the top panel is more optimistic than the bottom panel, it does agree to within 1-2 orders of magnitude over the range of parameters considered. We therefore consider the distinguishability criterion sufficient for making qualitative predictions and we will use this again in future sections.

These constraints are considerably stronger than the limit of $\lesssim 3 \times 10^{-15}$ placed with GW170817 [20]. This can be understood by remembering that this limit was based off of a time delay of ~ 5 seconds. However, a shift of even milliseconds in a gravitational-wave signal can be observable with matched-filtering and so we are able to probe much smaller values of δc_{GW} .

The LVK collaboration papers have also considered a variable gravitational-wave speed in terms of a “modified dispersion relation” [103, 111–114]. Bounds in these papers have not been directly quoted in terms of δc_{GW} . However, it is possible to translate between the constraining power on, for example, the graviton mass quoted in these papers and infer the implied constraining power for δc_{GW} ¹². The LVK analyses only compute bounds at specific values of σ , and do not consider σ values larger than 1. However, the results from analysing GW170817 data are compatible with our results, in regions where our analyses overlap [103]. Tighter bounds on the graviton mass have been placed on the LVK catalog using 43 confident binary black hole mergers in [114]. If this data were used to place bounds on c_{GW} it would result in bounds that are around two orders of magnitude tighter than those quoted here. This further backs up the main point of this section, which is that ground based observations of gravitational-wave mergers can place, and indeed have placed, very tight constraints on c_{GW} in the $\sim 10 - 1000\text{Hz}$ region.

V. PROBING c_{GW} IN THE LISA BAND

In the previous section we have demonstrated that we can place much tighter constraints upon deviations from general relativity in the LVK band if we assume a model where the speed of gravity diverges from the speed of light, but varies as a function of frequency. Even a very small variation as a function of frequency can cause a measurable frequency-dependent delay in arrival time in the observed gravitational-wave signal. Similar tests would also be possible for observations in the 1mHz - 100mHz with future space-based observatories, such as LISA [60] and TianQin [61]. Here we focus on the LISA observatory. Perhaps the most useful astrophysical source of gravitational waves for probing deviations from general relativity with LISA is the merger of two supermassive black holes. Such systems would have very large signal-to-noise ratio, would have relatively small mass ratios—where

reliability of waveform models is highest—and would cover a broad range of frequencies in the scale of O(few years) that LISA might observe such a source [115, 116].

Within the LISA context, bounds on δc_{GW} have previously been considered in two different settings. First, [51] investigated testing a frequency-independent δc_{GW} in the LISA band with a multi-messenger observation akin to GW170817. They forecasted a resulting bound $|\delta c_{\text{GW}}| \lesssim 10^{-12}$ in the event of a non-detection. As before, here we instead focus on candidate signatures of a frequency-dependent δc_{GW} and (given our findings in the LVK band above) expect to place significantly stronger bounds on such a signal. Secondly, while this paper was being completed [52] also investigated a frequency-dependent c_{GW} in the LISA band, similarly motivated by the observation of [53] that a frequency-dependent c_{GW} can lead to interesting phenomenology close to the LISA band and exploring its effect on waveform models and on (forecasted) parameter constraints. In terms of δc_{GW} constraints, their results are driven by redshift-induced frequency dependence (e.g. that the frequency of a monochromatic wave differs at the source and at the observer in an expanding Universe). This effect also is a generic consequence of a frequency-dependent c_{GW} and [52] uses this to place bounds on $|\delta c_{\text{GW}}| \lesssim 10^{-4}$. Here we show that these bounds can be improved by several orders of magnitude, more specifically to $|\delta c_{\text{GW}}| \lesssim 10^{-17}$, by considering the effects of $c_{\text{GW}} \neq c$ outlined in section III.

To demonstrate the potential capability of LISA to observe such effects we again use the distinguishability criterion introduced in the previous section. Here we consider a system with a pair of black holes both having a mass of $4.154 \times 10^6 M_{\odot}$ (the mass of the black hole at the centre of the Milky Way). We situate the system at a distance of 1 Gpc, which we take to be at a redshift of 0.20. We assume that the sky position and orientation of the system is such that it will induce the optimal response for the LISA detector and we assume that we observe the system from an initial gravitational wave frequency of $5 \times 10^{-5}\text{Hz}$, corresponding to roughly 1.5 months before merger, the period in which the majority of the signal power would be accrued. We model the LISA sensitivity curve using the LISA Sensitivity code¹³. Such a system would be recovered with a signal-to-noise ratio of around 5000 with LISA. It is possible that the transition frequency would occur within the LISA band of observation, so rather than modelling δc_{GW} as an asymptoting function, we use the 3-parameter model defined earlier in equation 10. We then, as a function of the transition frequency (f_{\star}) and the steepness of the transition (α), predict the values of $\delta c_{\text{GW}}^{(0)}$ that would be distinguishable from a signal modelled assuming GR.

The result of this can be seen in Figure 3. We can see that in the absence of a detection of a deviation from GR with such an observation, it would be possible to place very tight bounds over a large range of the parameter space that we consider. However, if c_{GW} has a steep transition with a transition

¹² We thank Nathan Johnson-McDaniel for pointing this out to us and for discussions about how the LVK results compare to our Figure 2.

¹³ https://github.com/ExtremeGravityInstitute/LISA_Sensitivity

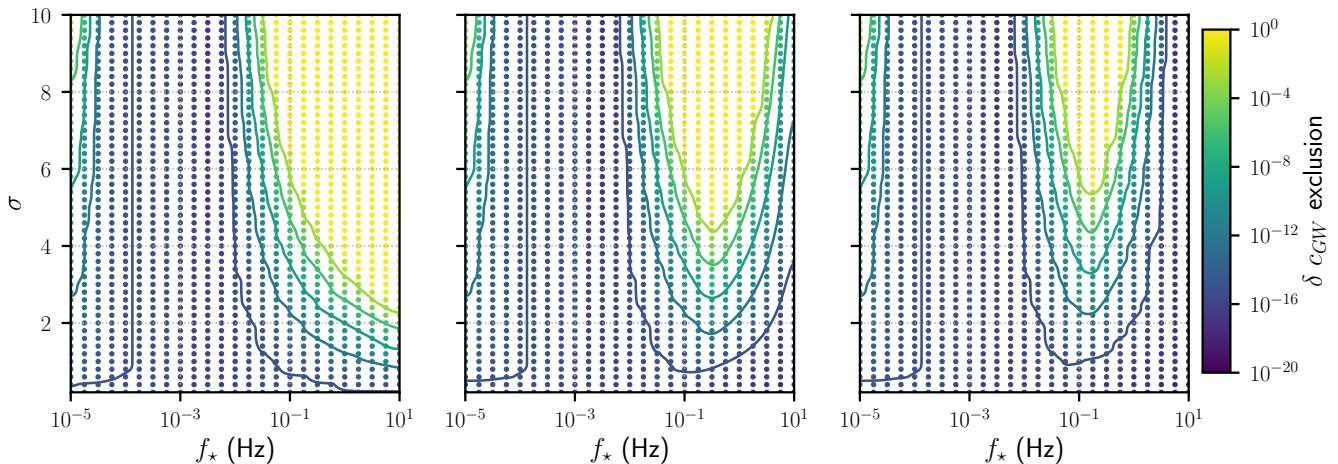


FIG. 3. The values of $\delta c_{\text{GW}}^{(0)}$ that would be distinguishable from a purely GR signal, as a function of the transition frequency (f_*) and the steepness of the transition (α). (Left) This is computed assuming a single LISA observation of a system of two supermassive black holes each having a mass of $4.154 \times 10^6 M_\odot$ at a distance of 1Gpc. (Middle) Computed assuming the combination of an LVK observation of a GW170817-like source and a single LISA observation of two supermassive black holes. (Right) Computed assuming the combination of an ET observation of a GW170817-like source and a single LISA observation of two supermassive black holes. In all cases contour lines correspond to $\delta c_{\text{GW}}^{(0)} = 10^{-3}, 10^{-6}, 10^{-9}, 10^{-12}$ and 10^{-15} .

frequency above 0.01 to 0.1Hz it would produce a signal in LISA that looks almost identical to a purely GR signal. It is important to remember that the detectability criterion we apply here was demonstrated to be optimistic by 1 to 2 orders of magnitude in the LVK band, and we might expect a similar behaviour here as well. Nevertheless, this will not affect the main features of our results shown in Figure 3. In this context also note that the bounds forecasted here are for a single source and, from the analogous LVK band discussion in the previous section, one may expect these bounds to improve in a similar manner when considering a catalog of LISA observations.

VI. PROBING c_{GW} WITH JOINT LVK/LISA OBSERVATIONS

It is interesting to compare how the bounds placed from simulated observations in the LVK band would combine with analogous bounds in the LISA band. If we re-compute our approximate bounds on c_{GW} used in Figure 2 in terms of the 3 parameters used in the previous section, it is easy to combine these plots and produce a visualization of the area of parameter space that would be excluded from observations in both bands. This can be seen in Figure 3. We can see that this combined exclusion includes much tighter constraints at larger values of the transition frequency, and would place very strong constraints for $\sigma < 2$ over the full range of transition frequencies considered. However, it would still permit cases where the transition frequency is between the two bounds (around 0.1 to 1 Hz) with a very steep transition curve. For completeness, we also show in Figure 3 how the constraints would improve with the observation of a GW170817-like source with the Einstein Telescope. Finally, we also in-

clude in Appendix D the uncombined exclusions, with only an LVK or ET observation of a GW170817-like source. Indeed, there we see that LVK band observations by themselves already strongly constrain δc_{GW} throughout the LISA band for $\sigma = 1$.

In addition to observations made with only ground-based, or only with space-based observatories, it will be possible, in the coming decades, to observe a gravitational-wave source *both* with ground-based and space-based observatories. This was first explored in [95] where it was demonstrated that a GW150914-like merger would be observable to LISA in the years before it merged in the ground-based observation window. Such *multi-band* observations offer the ability to perform particularly stringent tests of general relativity from observations of sources over a wide range of frequencies. In particular, consider the case that c_{GW} asymptotes to 1 before entering the ground-based observation window, and c_{GW} asymptotes to a constant $c_{\text{GW}}(0) \neq c$ in the LISA band of observation (at levels of accuracy sufficient to evade the detection of any frequency-dependence in the LVK and LISA bands themselves – see previous sections). Such a deviation would not be directly observable in either band, but in the gap between the signal leaving the LISA band and being observed in the LVK band there would be a shift in the travel time required for the signal to reach an observer. Relating this to our model fit to equation 10 this would require a large value of σ with f_* in the frequency gap between the LISA and LVK bands, which is the region that is poorly constrained in Figure 3.

If we consider GW150914 at a distance of 400Mpc, the travel time, in the Earth’s reference frame, for the signal to reach the Earth is 4×10^{16} seconds. Then, as with the previous cases, we can see that even very tiny changes in c_{GW} will produce large variations in the arrival time. To produce time shifts of ~ 10000 seconds—roughly the accuracy at which an

observation in the LISA band would be able to constrain the merger time as predicted in [98]¹⁴—would require $|\delta c_{\text{GW}}| = 3 \times 10^{-13}$. To produce time shifts of ~ 10 seconds—as predicted in [95–97]—would require $|\delta c_{\text{GW}}| = 3 \times 10^{-16}$. More generally speaking, if in the future the merger time in the LVK band can be predicted with an accuracy of $\sim 10^x$ seconds from LISA band observations, $\delta c_{\text{GW}} \sim 10^{-14+x-y}$ will be discernible for a source at 10^y Mpc.

An interesting observation can be made when considering larger values of $|\delta c_{\text{GW}}|$. In particular the time delay due to $|\delta c_{\text{GW}}|$ changing between the LISA and LVK bands can quickly become very large. A value of only $|\delta c_{\text{GW}}| = 8 \times 10^{-10}$ is required before the time delay is larger than a year. In such cases, with a subluminal c_{GW} , we might observe the signal with LISA at *the same time* as the signal arriving at ground based observatories. For values of $|\delta c_{\text{GW}}|$ that are much larger than this, we would not observe a multi-band signal at all, and indeed the absence of multi-band signals, when such observations are expected, could be an indicator of $|\delta c_{\text{GW}}|$ being large in the LISA band. With existing upper bounds on c_{GW} relevant for the LISA band imposing $|\delta c_{\text{GW}}| \lesssim 10^{-2}$ [14], this means there is in principle a window $|\delta c_{\text{GW}}| \sim 10^{-8} - 10^{-2}$ for which, given a sufficiently fast transition in between the LVK and LISA bands, the absence of multi-band signals would be the main signature in near-future measurements. This would also be an especially interesting target for proposed future experiments targeting this intermediate region, such as AEDGE [117]. Finally note that, while this draft was in internal review, we were made aware of ongoing work [99] that will also explore similar multiband constraints.

VII. CONCLUSIONS

Summary: In this paper we have explored how frequency-dependent transitions in the speed of gravitational waves c_{GW} – a generic consequence in large classes of dark energy theories – can be constrained by current and future observations in the LIGO/Virgo/KAGRA (LVK) band, in the LISA band and with joint observations in both bands. Since such dark energy-related transitions naturally occur close to those two bands, the observations place powerful constraints on c_{GW} . We would like to highlight the following key results:

- We find that deviations away from $c_{\text{GW}} = c$ can be constrained down to a level of $|\delta c_{\text{GW}}| \sim 10^{-17}$ in *both* the LVK *and* LISA bands even for mild frequency-dependence, much stronger than existing bounds for frequency-independent c_{GW} from GW170817 or indeed analogous forecasted bounds for multi-messenger observations in the LISA band [51]. Our constraints are driven by c_{GW} -induced frequency-dependent time shifts

in the observed signals and we have discussed in detail how they depend on the precise frequency(-ies) associated with the transition as well as on its functional form. Fig. 3 summarises the main constraints we find.

- We have identified a class of interesting very fast transitions taking place around frequencies of $\sim 10^{-2} - 10$ Hz, which can almost completely evade the aforementioned bounds when they proceed sufficiently quickly¹⁵. However, joint observations of sources visible in both LVK and LISA bands would be able to either: 1) constrain $|\delta c_{\text{GW}}| \lesssim 10^{-15}$, when LVK observations ‘see’ sources at the times expected from prior LISA observations of the same sources within expected uncertainties (note that this constraint can weaken to $|\delta c_{\text{GW}}| \lesssim 10^{-12}$ for more pessimistic forecasted uncertainties – see section VI for details), 2) measure $|\delta c_{\text{GW}}|$ anywhere in the range $|\delta c_{\text{GW}}| \sim 10^{-15} - 10^{-9}$, or 3) indicate that $|\delta c_{\text{GW}}| \sim 10^{-8} - 10^{-2}$, when LVK observations do not ‘see’ any expected counterparts for sources expected from prior LISA observations within $\mathcal{O}(\text{years})$.
- As a precursor for deriving these constraints, we have constructed a number of theoretically well-motivated templates for a fiducial frequency-dependent c_{GW} . Underlying most of our results is a simple three-parameter ansatz that captures the essential features of candidate transitions (see section II), but we collect a discussion of how to construct more sophisticated templates for future analyses in appendix B.

Implications for dark energy: In the immediate aftermath of GW170817 the consequences of tight bounds on $c_{\text{GW}} - |\delta c_{\text{GW}}| \lesssim 10^{-15}$ – on dark energy theories were explored in detail (see e.g. [2–5] and references therein), assuming these bounds can simply be ported to much lower cosmological frequencies. The resulting conclusions would be significantly more robust in the presence of an analogous precision measurement at LISA frequencies, as discussed and forecasted here. This is because we can consistently describe both cosmological and LISA scales in dark energy theories that lead to $c_{\text{GW}} \neq c$ on cosmological scales, while this is much more challenging for LVK scales [53].

In the context of Horndeski gravity explored in this paper, a tight bound on δc_{GW} from LISA would therefore firmly reduce the set of surviving scalar-tensor dark energy theories to [2–5] (also see [6–16] for closely related prior work)

$$\mathcal{L} = G_2(\phi, X) + G_3(\phi, X)\square\phi + G_4(\phi)R, \quad (19)$$

where the G_i are free functions of the scalar ϕ and its first derivative via $X \equiv -\frac{1}{2}\nabla_\mu\phi\nabla^\mu\phi$. Conversely, within the Horndeski context a detection of a non-zero δc_{GW} would constitute a measurement of significant G_4 and/or G_5 interactions

¹⁴ We remind the reader that there are inconsistent predictions of the ability to measure the arrival time of a signal in the LVK band with LISA, as we discussed in section III B

¹⁵ In terms of a power law scaling, this e.g. means $c_{\text{GW}} = c$ is approached at large frequencies as $f^{-2\sigma}$, where $\sigma \gtrsim 5$.

contributing to c_{GW} . Note that, by constraining the templates discussed here and in the event of a detection of non-zero δc_{GW} , not only would we obtain information about δc_{GW} itself and hence the value of c_{GW} on cosmological scales, but also about the f_* and σ parameters detailed in section II. f_* encodes information about the energy/frequency-scale associated with a UV completion for dark energy, while σ encodes information about the specific novel physics and interactions entailed by such a candidate UV completion.

Implications for future gravitational wave searches:

Throughout most of this paper our search for and constraints on c_{GW} with separate or combined, present and or forecasted LVK/LISA observations has been primarily motivated by large classes of dark energy theories that generically lead to a frequency-dependent c_{GW} in or close to those bands. What do our results imply beyond this dark energy-specific context? Ultimately a non-zero δc_{GW} would be evidence for novel gravitational interactions, new physics, that provide a non-trivial medium for gravitational waves to travel through. The template(s) we have worked with here do assume 1) an asymptotically constant c_{GW} at very low frequencies and 2) a frequency-dependent transition to $c_{\text{GW}} = c$ at some frequency f_* , whose form we have motivated by general field-theoretic arguments. Importantly, this means no further dark energy-specific input affects the templates themselves, so these can be implemented in future searches and offer a robust probe of any novel physics affecting c_{GW} in the LVK/LISA bands and (at least approximately) consistent with the above two assumptions, whether dark energy-related or otherwise.

ACKNOWLEDGMENTS

We especially thank Nathan Johnson-McDaniel and Scott Melville for several helpful discussions and shared insights. We also thank Tessa Baker, Anson Chen, Claudia de Rham, Macarena Lagos, Eugene Lim, Mauro Pieroni, Anand Sengupta and Gianmassimo Tasinato for useful discussions and comments on a draft. JN is supported by an STFC Ernest Rutherford Fellowship (ST/S004572/1). IH is supported by STFC grants ST/T000333/1 and ST/V005715/1. In deriving the results of this paper, we have used: xAct [118], PyCBC [119], LALSuite [101], emcee [109], numpy [120] and scipy [121].

DATA AVAILABILITY

All data used in this work, and the information necessary to fully reproduce any results and figures presented here, can be found at our data release page https://icg-gravwaves.github.io/probing_speed_of_gravity/.

OPEN ACCESS

This article is licensed under a Creative Commons Attribution 4.0 International License, which permits use, sharing, adapta-

tion, distribution and reproduction in any medium or format, as long as you give appropriate credit to the original author(s) and the source, provide a link to the Creative Commons licence, and indicate if changes were made. The images or other third party material in this article are included in the article's Creative Commons licence, unless indicated otherwise in a credit line to the material. If material is not included in the article's Creative Commons licence and your intended use is not permitted by statutory regulation or exceeds the permitted use, you will need to obtain permission directly from the copyright holder. To view a copy of this licence, visit <http://creativecommons.org/licenses/by/4.0/>.

Appendix A: c_{GW} in Horndeski gravity

In section II of the main text we focused on a specific example theory, namely (2). However, the key features relevant for this paper remain true for the much more general class of Horndeski theories, the most general Lorentz-invariant scalar-tensor action that gives rise to second order equations of motion. It is described by the following action

$$S_H = \int d^4x \sqrt{-g} \left\{ \sum_{i=2}^5 \mathcal{L}_i[\phi, g_{\mu\nu}] \right\}, \quad (\text{A1})$$

where we write the scalar-tensor Lagrangians \mathcal{L}_i (for a scalar ϕ and a massless tensor $g_{\mu\nu}$) as

$$\begin{aligned} \mathcal{L}_2 &= \Lambda_2^4 G_2, & \mathcal{L}_3 &= \frac{\Lambda_2^4}{\Lambda_3} G_3 \cdot [\Phi], \\ \mathcal{L}_4 &= \frac{\Lambda_2^8}{\Lambda_3^6} G_4 R + \frac{\Lambda_2^4}{\Lambda_3^2} G_{4,X} ([\Phi]^2 - [\Phi^2]), & (\text{A2}) \\ \mathcal{L}_5 &= \frac{\Lambda_2^8}{\Lambda_3^6} G_5 G_{\mu\nu} \Phi^{\mu\nu} - \frac{1}{6} \frac{\Lambda_2^4}{\Lambda_3^2} G_{5,X} ([\Phi]^3 - 3[\Phi][\Phi^2] + 2[\Phi^3]). \end{aligned}$$

Here we adopt a dimensionless definition $X \equiv -\frac{1}{2} \nabla_\mu \phi \nabla^\mu \phi / \Lambda_2^4$ for what is essentially the scalar kinetic term, and we have defined $\Phi^\mu_\nu \equiv \nabla^\mu \nabla_\nu \phi$. The G_i are dimensionless functions of ϕ/M_{Pl} and X , and $G_{i,\phi}$ and $G_{i,X}$ denote the partial derivatives of the G_i (with respect to these dimensionless arguments). Square brackets denote the trace, e.g. $[\Phi^2] \equiv \nabla^\mu \nabla_\nu \phi \nabla^\nu \nabla_\mu \phi$, and we have three mass scales: M_{Pl} , Λ_2 and Λ . In cosmology they are conventionally taken to satisfy $\Lambda_2^2 = M_{\text{Pl}} H_0$ and $\Lambda_3^3 = M_{\text{Pl}} H_0^2$, which ensures that all interactions can give $\mathcal{O}(1)$ contributions to the (cosmological) background evolution. General Relativity is recovered when $G_2 = G_3 = G_5 = 0$ and $G_4 = 1$. Note that the example theory (2) effectively amounts to a minimal choice of G_2 and G_4 , while $G_5 = g(\phi)$ and $G_3 = 0$. For the general Horndeski theory(A2), one can then work out the effect on c_{GW} and find

$$\alpha_T = 2 \frac{X}{M^2} \left[2G_{4,X} - 2G_{5,\phi} - \left(\frac{\ddot{\phi}}{H_0^2} - \frac{\dot{\phi}H}{H_0^2} \right) G_{5,X} \right]. \quad (\text{A3})$$

Here $M^2/2 = G_4 - 2XG_{4,X} + XG_{5,\phi} - \frac{\dot{\phi}H}{H_0^2} XG_{5,X}$ is the so-called effective Planck mass (albeit dimensionless in the way

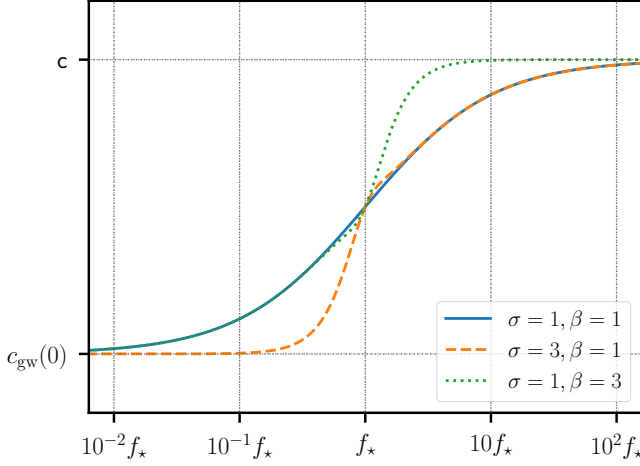


FIG. 4. The speed of gravitational waves, c_{GW} , as a function of frequency f for the extended template (B2). The different curves correspond to different choices of the ‘steepness’ parameters σ and β that control the asymptotic power law scalings of c_{GW} – see (B3). We have set $\gamma = 6$ for this example. This choice does not affect the asymptotes, but does determine how quickly the transition from a σ -dominated evolution to a β -dominated one occurs.

written here), H is the Hubble scale that measures the expansion of the Universe and satisfies $H = \dot{a}/a$ (where a is the scale factor of the Universe), and H_0 is the value of the Hubble scale today. Overdots denote time-derivatives with respect to proper time t and we recall that, on a cosmological background, the scalar ϕ is a function of time only, i.e. $\phi = \phi(t)$. From this it is clear that the presence of the scalar can affect c_{GW} through non-trivial G_4 and G_5 interactions. Conversely, if G_5 vanishes and G_4 is at most a function of ϕ (but not of its derivatives), then $\alpha_T = 0$ and there is no effect on c_{GW} and no deviation of this speed from the speed of light.

Appendix B: More c_{GW} templates

The c_{GW} template (10) we discussed in the main text is controlled by a single steepness parameter σ that controls both the small and large k asymptotes. The simplicity of the template results in a symmetric $k^{2\sigma}$ vs. $k^{-2\sigma}$ scaling for those asymptotes, but this can straightforwardly be refined by considering higher order (in the number of parameters) generalisations of this template, in particular ones that allow for different power law scalings in the asymptotic small and large frequency regimes. Here we will discuss how this can be done more explicitly.

Using the Θ_{\pm} functions defined in (9) we can define

$$\hat{\Theta}(\sigma, \beta, \gamma) \equiv \Theta_+(\gamma)\Theta_+(\beta) + \Theta_-(\gamma)\Theta_+(\sigma), \quad (\text{B1})$$

where it is understood that any Θ_{\pm} depends on f and f_* , but we no longer write this explicitly. We can now again build a template for c_{GW} as before, writing

$$c_{\text{GW}}(f) = c_{\text{GW}}^{(0)} + (c - c_{\text{GW}}^{(0)})\hat{\Theta}. \quad (\text{B2})$$

Note that we require $\gamma > \{\sigma, \beta\}$, but since it will not affect the large or small frequency asymptotes the precise value of γ is immaterial¹⁶. In this sense (B2) is really a four parameter template controlled by $\{c_{\text{GW}}(0), f_*, \sigma, \beta\}$. Investigating its asymptotic scalings explicitly, we find

$$\begin{aligned} k \ll k_* : & \quad c_{\text{GW}} - c_{\text{GW}}(0) \propto k^{2\sigma}, \\ k \gg k_* : & \quad c - c_{\text{GW}} \propto k^{-2\beta}. \end{aligned} \quad (\text{B3})$$

So σ and β control the relevant power law exponents in the large and small k regime, respectively, allowing different scalings in those two regimes. As discussed in the main text, a sufficiently fast (polynomial or otherwise) scaling as c_{GW} asymptotes back to unity is particularly important for ensuring consistency with measurements in the LVK band. So allowing for this parametric freedom for the large k scaling is especially relevant there, ultimately capturing one specific aspect of the lack of knowledge we have about the precise nature of any would-be UV completion of relevance for our analysis.

Finally, let us point out that the above template for asymmetric transitions is of course not unique. One example of an alternative template (albeit with less clean asymptotics) is a logistic/Verhulst function of the following type

$$\Theta_V(\sigma, \beta) \equiv 1 - \left(1 + (2^\beta - 1) \left(\frac{f}{f_*} \right)^\sigma \right)^{-1/\beta}, \quad (\text{B4})$$

from which we can build the template

$$c_{\text{GW}}(f) = c_{\text{GW}}^{(0)} + (c - c_{\text{GW}}^{(0)})\Theta_V. \quad (\text{B5})$$

Again we have introduced another parameter, β , that controls the asymmetry in the transition, allowing asymmetric scalings for small and large k in the transition.

Appendix C: Intrinsic source evolution with non-constant c_{GW}

In this appendix we would like to understand how a non-constant c_{GW} affects GW emission and propagation in the source frame, in particular how the intrinsic evolution of (and power emitted by) a binary system is affected if c_{GW} deviates from its GR prediction. We will compute this at leading, 0-PN, order, to demonstrate that these effects exist, but are negligible in our work. Higher order corrections would be needed if these effects were important. Closely following [14, 122], we can write the quadratic action for the standard metric tensor perturbations γ as

$$S_h = \frac{1}{64\pi G_{\text{GW}}} \int d^4x (\dot{\gamma}_j \dot{\gamma}^{jj} - k^2 c_{\text{GW}}^2 \gamma_j \gamma^{jj}), \quad (\text{C1})$$

¹⁶ Nevertheless note that it does affect the detailed transition evolution around f_* . Since those details are of lesser importance for the phenomenology investigated throughout this paper, we leave a more precise investigation of their effects to future work.

where G_{GW} denotes the effective gravitational ‘constant’ G seen by these tensor perturbations. We can then express the instantaneous power emitted as

$$\frac{dE}{dt} = \frac{r^2 c^4}{32\pi c_{\text{GW}} G_{\text{GW}}} \int d\Omega \langle \partial_t \gamma_{ij} \partial_t \gamma_{ij} \rangle, \quad (\text{C2})$$

where we integrate over solid angle Ω and average over a region of spacetime much larger than the GW wavelength (denoted by $\langle \dots \rangle$). In order to use the above we furthermore solve for the amplitude γ_{ij} of the radiated GWs by performing a multipole expansion and working to lowest (quadrupole) order in velocity. Solving the linearised Einstein equation and proceeding along the usual Green’s function solution (see e.g. [122]), we recover the expression [14]

$$[\gamma_{ij}]_{\text{quad}} = \frac{2G_{\text{GW}}}{r c^4} \ddot{Q}_{ij}^{TT} \left(t - \frac{r}{c_{\text{GW}}} \right), \quad (\text{C3})$$

at leading order in velocity. Here we have defined the usual quadrupole moment $Q^{ij} \equiv M^{ij} - \frac{1}{3} \delta^{ij} M^k_k$ in terms of the momenta of T^{00}/c^2 , M . Note that, in performing the above computation it is important that the time it takes for a GW to traverse the source is negligible compared to the time variation scale of c_{GW} , which allows us to effectively treat c_{GW} as constant in the relevant integrals.

Now we would like to work out the *total* power emitted, starting from (C2). Re-arranging, we obtain

$$\frac{dP}{d\Omega} = \frac{r^2 c^4}{32\pi c_{\text{GW}} G_{\text{GW}}} \langle \partial_t \gamma_{ij} \partial_t \gamma_{ij} \rangle = \frac{G_{\text{GW}}}{8\pi c_{\text{GW}} c^4} \langle \ddot{Q}_{ij}^{TT} \ddot{Q}_{ij}^{TT} \rangle. \quad (\text{C4})$$

Here $P \equiv dE/dt$ and we have substituted for γ_{ij} using (C3). Instead of writing this in terms of its transverse-traceless projection Q_{ij}^{TT} , we would like to express this in terms of the quadrupole moment of the source Q_{ij} itself. Doing so and integrating over solid angle again, we find the total (quadrupolar) power emitted (at a given time)

$$P_{\text{quad}} = \frac{G_{\text{GW}}}{5c_{\text{GW}} c^4} \langle \ddot{Q}_{kl} \ddot{Q}_{mn} \rangle, \quad (\text{C5})$$

again recovering the result from [14]. We emphasise that this expression holds for a time/frequency-varying c_{GW} , since it is the total power emitted at a given time/frequency, but care needs to be taken when integrating this expression to e.g. obtain the total energy emitted throughout the evolution.

We now focus on a circular inspiral and explicitly work out the power emitted in terms of the parameters describing this system. Establishing some notation, we have

$$\omega_s^2 = \frac{G_N m}{R^3}, \quad \omega_{\text{GW}} = 2\omega_s, \quad f_{\text{GW}} = \frac{\omega_{\text{GW}}}{2\pi}, \quad M_c = \mu^{3/5} m^{2/5}, \quad (\text{C6})$$

where we recall that

$$\mu \equiv \frac{m_1 m_2}{m_1 + m_2}, \quad m \equiv m_1 + m_2, \quad (\text{C7})$$

and m_1 and m_2 are the masses of the two compact objects constituting the inspiralling binary in question. Importantly, in (C6), note that the expression for ω_s is effectively Kepler’s law and so the appropriate gravitational coupling constant here is G_N , i.e. the gravitational constant that enters in the Poisson equation and which is generically different from G_{GW} . In this setup we can solve for γ and find

$$\gamma_{\times}(t, \theta, \phi) = \frac{4G_{\text{GW}} \mu \omega_s^2 R^2}{r c^3} c_{\text{GW}} \cos \theta \sin(2\omega_s t_{\text{ret}} + 2\phi) \quad (\text{C8})$$

where we note the factor of G_{GW} that enters following on from (C3) and we only show the \times polarisation for brevity here – see (3.330) and (3.331) in [122] for an analogous $+$ polarisation expression, which can be adapted along the same lines. Note that t_{ret} has an implicit c_{GW} dependence as well. Now using (C6) to replace R with ω_s and explicitly introducing the chirp mass, we can write

$$\gamma_{\times}(t, \theta, \phi) = \frac{G_{\text{GW}} c}{G_N c_{\text{GW}}} \frac{4}{r} \left(\frac{G_N M_c}{c^2} \right)^{5/3} \left(\frac{\pi f_{\text{GW}}}{c} \right)^{2/3} \cdot \cos \theta \sin(2\omega_s t_{\text{ret}} + 2\phi). \quad (\text{C9})$$

The first fraction encodes all dark energy-related modifications we consider here, while everything that remains is as in standard GR. Finally, we can follow the same logic as above and compute the resulting total power emitted at any given point in time

$$P = \frac{G_{\text{GW}} c}{G_N c_{\text{GW}}} \frac{32c^5}{5G_N} \left(\frac{G_N M_c \omega_{\text{GW}}}{2c^3} \right)^{10/3}. \quad (\text{C10})$$

The power lost to gravitational radiation will be equal to loss of orbital energy, and, assuming Keplerian orbits, this can be expressed in terms of M_c and ω as [122]

$$P = -\frac{dE_{\text{orbit}}}{dt} = \frac{2}{3} \left(\frac{G_N^2 M_c^{5/3}}{32} \right)^{1/3} \omega^{-1/3} \dot{\omega}. \quad (\text{C11})$$

This can be rearranged in terms of $\dot{\omega}$ to give

$$\dot{\omega}(t) = \left(\frac{G_{\text{GW}} c}{G_N c_{\text{GW}}} \right) \frac{3456^{1/3}}{5} \left(\frac{G_N M_c}{c^3} \right)^{5/3} \omega^{11/3}. \quad (\text{C12})$$

In the generic case we are considering where c_{GW} and G_{GW} depend on frequency we cannot simplify further without specifying that dependency. In the simple case that $c_{\text{GW}} = 1$ and $G_{\text{GW}} = G_N$ the extra term on the right hand side vanishes and this collapses to the standard 0-PN GR solution. In the case where c_{GW} and G_{GW} deviate from the GR values but are constant over the range of observation this can be integrated analytically and rearranged to find $h_+(t)$ and $h_{\times}(t)$. In this case we find that both the phasing evolution and the overall amplitude depend on c_{GW} and G_{GW} , but do so in a way that is degenerate with chirp mass. Therefore a signal emitted in such a model would appear to be consistent with general relativity, but the recovered measurement of the chirp mass would be

offset from the true value – also see [92] for a related discussion of phase shifts and degeneracies. In the case of a general solution for $c_{\text{GW}}(\omega)$ and $G_{\text{GW}}(\omega)$ this could be integrated numerically to find a model of the emitted waveform.

In the above we have kept G_{GW} and G_N , i.e. two different gravitational coupling constants for gravitational waves and for matter, generic. However, within the context of (A2) and inside a screened regime as is relevant for the emission of gravitational waves considered here, these are found to satisfy $G_N/G_{\text{GW}} = c_{\text{GW}}^2/c^2$ [14]¹⁷. So here any modification of (C12) away from its GR limit will be controlled by a single, dimensionless parameter: c_{GW}/c . However, bounds obtained from this effect will be significantly weaker than the ones discussed in the main text. Compare the $|\delta c_{\text{GW}}| \lesssim 10^{-2}$ bound obtained by [14] from the Hulse-Taylor binary using analogous reasoning with the $|\delta c_{\text{GW}}| \lesssim 10^{-17}$ and better constraints discussed

in the main text. We therefore do not pursue bounds from this effect further here.

Appendix D: Constraints using only LVK or ET observations

In Figure 3 we showed the potential constraints that could be placed on c_{GW} when combining an observation of a supermassive black hole merger with LISA with a single observation of a GW170817-like source with LVK/ET. For completeness, in Figure 5, we also show what the constraints would look like if *only* considering a single GW170817-like source observed with either LVK or ET, alongside the constraints from LISA alone as comparison.

-
- [1] Planck Collaboration, N. Aghanim *et al.*, “Planck 2018 results. VI. Cosmological parameters,” *Astron. Astrophys.* **641** (2020) A6, arXiv:1807.06209 [astro-ph.CO].
- [2] T. Baker, E. Bellini, P. G. Ferreira, M. Lagos, J. Noller, and I. Sawicki, “Strong constraints on cosmological gravity from GW170817 and GRB 170817A,” *Phys. Rev. Lett.* **119** (2017) no. 25, 251301, arXiv:1710.06394 [astro-ph.CO].
- [3] P. Creminelli and F. Vernizzi, “Dark Energy after GW170817 and GRB170817A,” *Phys. Rev. Lett.* **119** (2017) no. 25, 251302, arXiv:1710.05877 [astro-ph.CO].
- [4] J. Sakstein and B. Jain, “Implications of the Neutron Star Merger GW170817 for Cosmological Scalar-Tensor Theories,” *Phys. Rev. Lett.* **119** (2017) no. 25, 251303, arXiv:1710.05893 [astro-ph.CO].
- [5] J. M. Ezquiaga and M. Zumalacárregui, “Dark Energy After GW170817: Dead Ends and the Road Ahead,” *Phys. Rev. Lett.* **119** (2017) no. 25, 251304, arXiv:1710.05901 [astro-ph.CO].
- [6] L. Amendola, M. Kunz, M. Motta, I. D. Saltas, and I. Sawicki, “Observables and unobservables in dark energy cosmologies,” *Phys. Rev.* **D87** (2013) no. 2, 023501, arXiv:1210.0439 [astro-ph.CO].
- [7] L. Amendola, G. Ballesteros, and V. Pettorino, “Effects of modified gravity on B-mode polarization,” *Phys. Rev.* **D90** (2014) 043009, arXiv:1405.7004 [astro-ph.CO].
- [8] C. Deffayet, O. Pujolas, I. Sawicki, and A. Vikman, “Imperfect Dark Energy from Kinetic Gravity Braiding,” *JCAP* **1010** (2010) 026, arXiv:1008.0048 [hep-th].
- [9] E. V. Linder, “Are Scalar and Tensor Deviations Related in Modified Gravity?,” *Phys. Rev.* **D90** (2014) no. 8, 083536, arXiv:1407.8184 [astro-ph.CO].
- [10] M. Raveri, C. Baccigalupi, A. Silvestri, and S.-Y. Zhou, “Measuring the speed of cosmological gravitational waves,” *Phys. Rev.* **D91** (2015) no. 6, 061501, arXiv:1405.7974 [astro-ph.CO].
- [11] I. D. Saltas, I. Sawicki, L. Amendola, and M. Kunz, “Anisotropic Stress as a Signature of Nonstandard Propagation of Gravitational Waves,” *Phys. Rev. Lett.* **113** (2014) no. 19, 191101, arXiv:1406.7139 [astro-ph.CO].
- [12] L. Lombriser and A. Taylor, “Breaking a Dark Degeneracy with Gravitational Waves,” *JCAP* **1603** (2016) no. 03, 031, arXiv:1509.08458 [astro-ph.CO].
- [13] L. Lombriser and N. A. Lima, “Challenges to Self-Acceleration in Modified Gravity from Gravitational Waves and Large-Scale Structure,” *Phys. Lett.* **B765** (2017) 382–385, arXiv:1602.07670 [astro-ph.CO].
- [14] J. Beltran Jimenez, F. Piazza, and H. Velten, “Evading the Vainshtein Mechanism with Anomalous Gravitational Wave Speed: Constraints on Modified Gravity from Binary Pulsars,” *Phys. Rev. Lett.* **116** (2016) no. 6, 061101, arXiv:1507.05047 [gr-qc].
- [15] D. Bettoni, J. M. Ezquiaga, K. Hinterbichler, and M. Zumalacárregui, “Speed of Gravitational Waves and the Fate of Scalar-Tensor Gravity,” *Phys. Rev.* **D95** (2017) no. 8, 084029, arXiv:1608.01982 [gr-qc].
- [16] I. Sawicki, I. D. Saltas, M. Motta, L. Amendola, and M. Kunz, “Nonstandard gravitational waves imply gravitational slip: On the difficulty of partially hiding new gravitational degrees of freedom,” *Phys. Rev.* **D95** (2017) no. 8, 083520, arXiv:1612.02002 [astro-ph.CO].
- [17] LIGO Scientific, Virgo Collaboration, B. Abbott *et al.*, “GW170817: Observation of Gravitational Waves from a Binary Neutron Star Inspiral,” *Phys. Rev. Lett.* **119** (2017) no. 16, 161101, arXiv:1710.05832 [gr-qc].
- [18] A. Goldstein *et al.*, “An Ordinary Short Gamma-Ray Burst with Extraordinary Implications: Fermi-GBM Detection of GRB 170817A,” *Astrophys. J. Lett.* **848** (2017) no. 2, L14, arXiv:1710.05446 [astro-ph.HE].
- [19] V. Savchenko *et al.*, “INTEGRAL Detection of the First Prompt Gamma-Ray Signal Coincident with the Gravitational-wave Event GW170817,” *Astrophys. J. Lett.* **848** (2017) no. 2, L15, arXiv:1710.05449 [astro-ph.HE].
- [20] LIGO Scientific, Virgo, Fermi-GBM, INTEGRAL Collaboration, B. P. Abbott *et al.*, “Gravitational Waves and Gamma-rays from a Binary Neutron Star Merger: GW170817 and GRB 170817A,” *Astrophys. J. Lett.* **848** (2017) no. 2, L13, arXiv:1710.05834 [astro-ph.HE].

¹⁷ This relationship may break down once approaching the cutoff of the cosmological theory close to Λ , so care needs to be taken if this is to be modelled in detail.

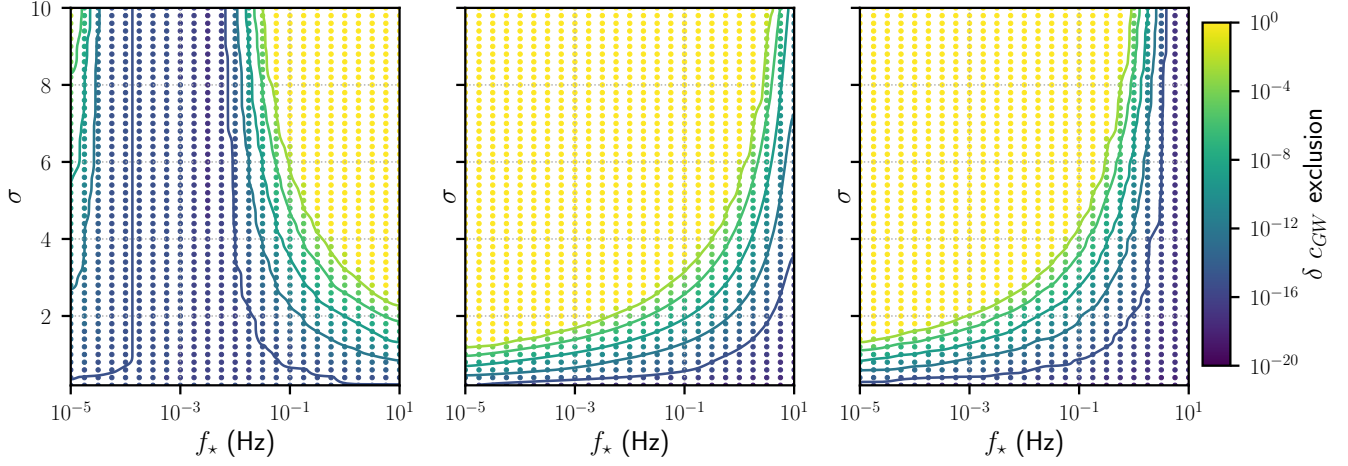


FIG. 5. The values of $\delta c_{\text{GW}}^{(0)}$ that would be distinguishable from a purely GR signal, as a function of the transition frequency (f_*) and the steepness of the transition (α). (Left) This is computed assuming a single LISA observation of a system of two supermassive black holes each having a mass of $4.154 \times 10^6 M_\odot$ at a distance of 1 Gpc. (Middle) Computed assuming an LVK observation of a GW170817-like source. (Right) Computed assuming an ET observation of a GW170817-like source. In all cases contour lines correspond to $\delta c_{\text{GW}}^{(0)} = 10^{-3}, 10^{-6}, 10^{-9}, 10^{-12}$ and 10^{-15} .

- [21] B. P. Abbott *et al.*, “Multi-messenger Observations of a Binary Neutron Star Merger,” *Astrophys. J. Lett.* **848** (2017) no. 2, L12, [arXiv:1710.05833 \[astro-ph.HE\]](#).
- [22] C. de Rham and A. J. Tolley, “Speed of gravity,” *Phys. Rev. D* **101** (2020) no. 6, 063518, [arXiv:1909.00881 \[hep-th\]](#).
- [23] C. de Rham, S. Melville, and J. Noller, “Positivity bounds on dark energy: when matter matters,” *JCAP* **08** (2021) 018, [arXiv:2103.06855 \[astro-ph.CO\]](#).
- [24] J. Noller and A. Nicola, “Cosmological parameter constraints for Horndeski scalar-tensor gravity,” *Phys. Rev. D* **99** (2019) no. 10, 103502, [arXiv:1811.12928 \[astro-ph.CO\]](#).
- [25] E. Bellini, A. J. Cuesta, R. Jimenez, and L. Verde, “Constraints on deviations from Λ CDM within Horndeski gravity,” *JCAP* **02** (2016) 053, [arXiv:1509.07816 \[astro-ph.CO\]](#). [Erratum: *JCAP* 06, E01 (2016)].
- [26] B. Hu, M. Raveri, N. Frusciante, and A. Silvestri, “Effective Field Theory of Cosmic Acceleration: an implementation in CAMB,” *Phys. Rev. D* **89** (2014) no. 10, 103530, [arXiv:1312.5742 \[astro-ph.CO\]](#).
- [27] M. Raveri, B. Hu, N. Frusciante, and A. Silvestri, “Effective Field Theory of Cosmic Acceleration: constraining dark energy with CMB data,” *Phys. Rev. D* **90** (2014) no. 4, 043513, [arXiv:1405.1022 \[astro-ph.CO\]](#).
- [28] J. Gleyzes, D. Langlois, M. Mancarella, and F. Vernizzi, “Effective Theory of Dark Energy at Redshift Survey Scales,” *JCAP* **1602** (2016) no. 02, 056, [arXiv:1509.02191 \[astro-ph.CO\]](#).
- [29] C. D. Kreisch and E. Komatsu, “Cosmological Constraints on Horndeski Gravity in Light of GW170817,” [arXiv:1712.02710 \[astro-ph.CO\]](#).
- [30] M. Zumalacárregui, E. Bellini, I. Sawicki, J. Lesgourgues, and P. G. Ferreira, “hi_class: Horndeski in the Cosmic Linear Anisotropy Solving System,” *JCAP* **1708** (2017) no. 08, 019, [arXiv:1605.06102 \[astro-ph.CO\]](#).
- [31] D. Alonso, E. Bellini, P. G. Ferreira, and M. Zumalacárregui, “Observational future of cosmological scalar-tensor theories,” *Phys. Rev. D* **95** (2017) no. 6, 063502, [arXiv:1610.09290 \[astro-ph.CO\]](#).
- [32] S. Arai and A. Nishizawa, “Generalized framework for testing gravity with gravitational-wave propagation. II. Constraints on Horndeski theory,” *Phys. Rev. D* **97** (2018) no. 10, 104038, [arXiv:1711.03776 \[gr-qc\]](#).
- [33] N. Frusciante, S. Peirone, S. Casas, and N. A. Lima, “The road ahead of Horndeski: cosmology of surviving scalar-tensor theories,” [arXiv:1810.10521 \[astro-ph.CO\]](#).
- [34] R. Reischke, A. S. Mancini, B. M. Schafer, and P. M. Merkel, “Investigating scalar-tensor-gravity with statistics of the cosmic large-scale structure,” [arXiv:1804.02441 \[astro-ph.CO\]](#).
- [35] A. Spurio Mancini, R. Reischke, V. Pettorino, B. M. Schafer, and M. Zumalacárregui, “Testing (modified) gravity with 3D and tomographic cosmic shear,” *Mon. Not. Roy. Astron. Soc.* **480** (2018) 3725, [arXiv:1801.04251 \[astro-ph.CO\]](#).
- [36] J. Noller and A. Nicola, “Radiative stability and observational constraints on dark energy and modified gravity,” *Phys. Rev. D* **102** (2020) no. 10, 104045, [arXiv:1811.03082 \[astro-ph.CO\]](#).
- [37] S. Arai, P. Karmakar, and A. Nishizawa, “Cosmological evolution of viable models in the generalized scalar-tensor theory,” *Phys. Rev. D* **102** (2020) no. 2, 024003, [arXiv:1912.01768 \[gr-qc\]](#).
- [38] G. Brando, F. T. Falciano, E. V. Linder, and H. E. S. Velten, “Modified gravity away from a Λ CDM background,” *JCAP* **11** (2019) 018, [arXiv:1904.12903 \[astro-ph.CO\]](#).
- [39] R. Arjona, W. Cardona, and S. Nesseris, “Designing Horndeski and the effective fluid approach,” *Phys. Rev. D* **100** (2019) no. 6, 063526, [arXiv:1904.06294 \[astro-ph.CO\]](#).
- [40] M. Raveri, “Reconstructing Gravity on Cosmological Scales,” *Phys. Rev. D* **101** (2020) no. 8, 083524, [arXiv:1902.01366 \[astro-ph.CO\]](#).
- [41] L. Perenon, J. Bel, R. Maartens, and A. de la Cruz-Dombriz, “Optimising growth of structure constraints on modified

- gravity,” *JCAP* **06** (2019) 020, [arXiv:1901.11063 \[astro-ph.CO\]](#).
- [42] N. Frusciante and L. Perenon, “Effective field theory of dark energy: A review,” *Phys. Rept.* **857** (2020) 1–63, [arXiv:1907.03150 \[astro-ph.CO\]](#).
- [43] A. Spurio Mancini, F. Köhlinger, B. Joachimi, V. Pettorino, B. M. Schäfer, R. Reischke, E. van Uitert, S. Brieden, M. Archidiacono, and J. Lesgourgues, “KiDS + GAMA: constraints on horndeski gravity from combined large-scale structure probes,” *Mon. Not. Roy. Astron. Soc.* **490** (2019) no. 2, 2155–2177, [arXiv:1901.03686 \[astro-ph.CO\]](#).
- [44] A. Bonilla, R. D’Agostino, R. C. Nunes, and J. C. N. de Araujo, “Forecasts on the speed of gravitational waves at high z ,” *JCAP* **03** (2020) 015, [arXiv:1910.05631 \[gr-qc\]](#).
- [45] T. Baker and I. Harrison, “Constraining Scalar-Tensor Modified Gravity with Gravitational Waves and Large Scale Structure Surveys,” *JCAP* **01** (2021) 068, [arXiv:2007.13791 \[astro-ph.CO\]](#).
- [46] S. Joudaki, P. G. Ferreira, N. A. Lima, and H. A. Winther, “Testing Gravity on Cosmic Scales: A Case Study of Jordan-Brans-Dicke Theory,” [arXiv:2010.15278 \[astro-ph.CO\]](#).
- [47] J. Noller, L. Santoni, E. Trincerini, and L. G. Trombetta, “Scalar-tensor cosmologies without screening,” *JCAP* **01** (2021) 045, [arXiv:2008.08649 \[astro-ph.CO\]](#).
- [48] J. Noller, “Cosmological constraints on dark energy in light of gravitational wave bounds,” *Phys. Rev. D* **101** (2020) no. 6, 063524, [arXiv:2001.05469 \[astro-ph.CO\]](#).
- [49] D. Traykova, E. Bellini, P. G. Ferreira, C. García-García, J. Noller, and M. Zumalacárregui, “Theoretical priors in scalar-tensor cosmologies: Shift-symmetric Horndeski models,” *Phys. Rev. D* **104** (2021) no. 8, 083502, [arXiv:2103.11195 \[astro-ph.CO\]](#).
- [50] G. D. Moore and A. E. Nelson, “Lower bound on the propagation speed of gravity from gravitational Cherenkov radiation,” *JHEP* **09** (2001) 023, [arXiv:hep-ph/0106220](#).
- [51] T. B. Littenberg and N. J. Cornish, “Prospects for Gravitational Wave Measurement of ZTF J1539+5027,” *Astrophys. J. Lett.* **881** (2019) no. 2, L43, [arXiv:1908.00678 \[astro-ph.IM\]](#).
- [52] T. Baker *et al.*, “Measuring the propagation speed of gravitational waves with LISA,” [arXiv:2203.00566 \[gr-qc\]](#).
- [53] C. de Rham and S. Melville, “Gravitational Rainbows: LIGO and Dark Energy at its Cutoff,” *Phys. Rev. Lett.* **121** (2018) no. 22, 221101, [arXiv:1806.09417 \[hep-th\]](#).
- [54] **LIGO Scientific** Collaboration, J. Aasi *et al.*, “Advanced LIGO,” *Class. Quant. Grav.* **32** (2015) 074001, [arXiv:1411.4547 \[gr-qc\]](#).
- [55] **VIRGO** Collaboration, F. Acernese *et al.*, “Advanced Virgo: a second-generation interferometric gravitational wave detector,” *Class. Quant. Grav.* **32** (2015) no. 2, 024001, [arXiv:1408.3978 \[gr-qc\]](#).
- [56] **KAGRA** Collaboration, Y. Aso, Y. Michimura, K. Somiya, M. Ando, O. Miyakawa, T. Sekiguchi, D. Tatsumi, and H. Yamamoto, “Interferometer design of the KAGRA gravitational wave detector,” *Phys. Rev. D* **88** (2013) no. 4, 043007, [arXiv:1306.6747 \[gr-qc\]](#).
- [57] **KAGRA, LIGO Scientific, Virgo** Collaboration, B. P. Abbott *et al.*, “Prospects for observing and localizing gravitational-wave transients with Advanced LIGO, Advanced Virgo and KAGRA,” *Living Rev. Rel.* **21** (2018) no. 1, 3, [arXiv:1304.0670 \[gr-qc\]](#).
- [58] M. Punturo *et al.*, “The third generation of gravitational wave observatories and their science reach,” *Class. Quant. Grav.* **27** (2010) 084007.
- [59] D. Reitze *et al.*, “Cosmic Explorer: The U.S. Contribution to Gravitational-Wave Astronomy beyond LIGO,” *Bull. Am. Astron. Soc.* **51** (2019) no. 7, 035, [arXiv:1907.04833 \[astro-ph.IM\]](#).
- [60] **LISA** Collaboration, P. Amaro-Seoane *et al.*, “Laser Interferometer Space Antenna,” [arXiv:1702.00786 \[astro-ph.IM\]](#).
- [61] **TianQin** Collaboration, J. Luo *et al.*, “TianQin: a space-borne gravitational wave detector,” *Class. Quant. Grav.* **33** (2016) no. 3, 035010, [arXiv:1512.02076 \[astro-ph.IM\]](#).
- [62] G. W. Horndeski, “Second-order scalar-tensor field equations in a four-dimensional space,” *Int. J. Theor. Phys.* **10** (1974) 363–384.
- [63] C. Deffayet, X. Gao, D. A. Steer, and G. Zahariade, “From k-essence to generalised Galileons,” *Phys. Rev.* **D84** (2011) 064039, [arXiv:1103.3260 \[hep-th\]](#).
- [64] T. Kobayashi, M. Yamaguchi, and J. Yokoyama, “Generalized G-inflation: Inflation with the most general second-order field equations,” *Prog. Theor. Phys.* **126** (2011) 511–529, [arXiv:1105.5723 \[hep-th\]](#).
- [65] E. Bellini and I. Sawicki, “Maximal freedom at minimum cost: linear large-scale structure in general modifications of gravity,” *JCAP* **1407** (2014) 050, [arXiv:1404.3713 \[astro-ph.CO\]](#).
- [66] L. Berezhiani, G. Chkareuli, and G. Gabadadze, “Restricted Galileons,” *Phys. Rev.* **D88** (2013) 124020, [arXiv:1302.0549 \[hep-th\]](#).
- [67] K. Koyama, G. Niz, and G. Tasinato, “Effective theory for the Vainshtein mechanism from the Horndeski action,” *Phys. Rev. D* **88** (2013) 021502, [arXiv:1305.0279 \[hep-th\]](#).
- [68] S. Melville and J. Noller, “Positivity in the Sky: Constraining dark energy and modified gravity from the UV,” *Phys. Rev. D* **101** (2020) no. 2, 021502, [arXiv:1904.05874 \[astro-ph.CO\]](#).
- [69] H. Georgi, “Effective field theory,” *Ann. Rev. Nucl. Part. Sci.* **43** (1993) 209–252.
- [70] J. F. Donoghue, “Introduction to the effective field theory description of gravity,” in *Advanced School on Effective Theories*. 6, 1995. [arXiv:gr-qc/9512024](#).
- [71] C. P. Burgess, “Introduction to Effective Field Theory,” *Ann. Rev. Nucl. Part. Sci.* **57** (2007) 329–362, [arXiv:hep-th/0701053](#).
- [72] B. Ratra and P. J. E. Peebles, “Cosmological Consequences of a Rolling Homogeneous Scalar Field,” *Phys. Rev. D* **37** (1988) 3406.
- [73] C. Wetterich, “Cosmology and the Fate of Dilatation Symmetry,” *Nucl. Phys. B* **302** (1988) 668–696, [arXiv:1711.03844 \[hep-th\]](#).
- [74] P. G. Ferreira and M. Joyce, “Cosmology with a primordial scaling field,” *Phys. Rev. D* **58** (1998) 023503, [arXiv:astro-ph/9711102](#).
- [75] R. R. Caldwell, R. Dave, and P. J. Steinhardt, “Cosmological imprint of an energy component with general equation of state,” *Phys. Rev. Lett.* **80** (1998) 1582–1585, [arXiv:astro-ph/9708069](#).
- [76] C. Armendariz-Picon, T. Damour, and V. F. Mukhanov, “k -inflation,” *Phys. Lett.* **B458** (1999) 209–218, [arXiv:hep-th/9904075 \[hep-th\]](#).

- [77] J. Garriga and V. F. Mukhanov, “Perturbations in k-inflation,” *Phys. Lett.* **B458** (1999) 219–225, [arXiv:hep-th/9904176 \[hep-th\]](#).
- [78] C. Armendariz-Picon, V. F. Mukhanov, and P. J. Steinhardt, “A Dynamical solution to the problem of a small cosmological constant and late time cosmic acceleration,” *Phys. Rev. Lett.* **85** (2000) 4438–4441, [arXiv:astro-ph/0004134 \[astro-ph\]](#).
- [79] C. Armendariz-Picon, V. F. Mukhanov, and P. J. Steinhardt, “Essentials of k essence,” *Phys. Rev.* **D63** (2001) 103510, [arXiv:astro-ph/0006373 \[astro-ph\]](#).
- [80] M. A. Luty, M. Porrati, and R. Rattazzi, “Strong interactions and stability in the DGP model,” *JHEP* **09** (2003) 029, [arXiv:hep-th/0303116 \[hep-th\]](#).
- [81] A. Nicolis and R. Rattazzi, “Classical and quantum consistency of the DGP model,” *JHEP* **06** (2004) 059, [arXiv:hep-th/0404159 \[hep-th\]](#).
- [82] C. de Rham and A. J. Tolley, “DBI and the Galileon reunited,” *JCAP* **05** (2010) 015, [arXiv:1003.5917 \[hep-th\]](#).
- [83] C. Burrage, C. de Rham, D. Seery, and A. J. Tolley, “Galileon inflation,” *JCAP* **01** (2011) 014, [arXiv:1009.2497 \[hep-th\]](#).
- [84] C. de Rham and R. H. Ribeiro, “Riding on irrelevant operators,” *JCAP* **1411** (2014) no. 11, 016, [arXiv:1405.5213 \[hep-th\]](#).
- [85] D. Pirtskhalava, L. Santoni, E. Trincherini, and F. Vernizzi, “Weakly Broken Galileon Symmetry,” *JCAP* **1509** (2015) no. 09, 007, [arXiv:1505.00007 \[hep-th\]](#).
- [86] C. de Rham, G. Gabadadze, L. Heisenberg, and D. Pirtskhalava, “Nonrenormalization and naturalness in a class of scalar-tensor theories,” *Phys. Rev. D* **87** (2013) no. 8, 085017, [arXiv:1212.4128 \[hep-th\]](#).
- [87] G. Goon, K. Hinterbichler, A. Joyce, and M. Trodden, “Aspects of Galileon Non-Renormalization,” *JHEP* **11** (2016) 100, [arXiv:1606.02295 \[hep-th\]](#).
- [88] I. D. Saltas and V. Vitagliano, “Covariantly Quantum Galileon,” *Phys. Rev. D* **95** (2017) no. 10, 105002, [arXiv:1611.07984 \[hep-th\]](#).
- [89] L. Heisenberg and C. F. Steinwachs, “Geometrized quantum Galileons,” *JCAP* **02** (2020) 031, [arXiv:1909.07111 \[hep-th\]](#).
- [90] L. Heisenberg, J. Noller, and J. Zosso, “Horndeski under the quantum loupe,” *JCAP* **10** (2020) 010, [arXiv:2004.11655 \[hep-th\]](#).
- [91] G. Goon, S. Melville, and J. Noller, “Quantum corrections to generic branes: DBI, NLSM, and more,” *JHEP* **01** (2021) 159, [arXiv:2010.05913 \[hep-th\]](#).
- [92] S. Mirshekari, N. Yunes, and C. M. Will, “Constraining Generic Lorentz Violation and the Speed of the Graviton with Gravitational Waves,” *Phys. Rev. D* **85** (2012) 024041, [arXiv:1110.2720 \[gr-qc\]](#).
- [93] U. Sperhake, C. J. Moore, R. Rosca, M. Agathos, D. Gerosa, and C. D. Ott, “Long-lived inverse chirp signals from core collapse in massive scalar-tensor gravity,” *Phys. Rev. Lett.* **119** (2017) no. 20, 201103, [arXiv:1708.03651 \[gr-qc\]](#).
- [94] J. C. Aurrekoetxea, P. G. Ferreira, K. Clough, E. A. Lim, and O. J. Tattersall, “Where is the ringdown? Reconstructing quasinormal modes from dispersive waves,” [arXiv:2205.15878 \[gr-qc\]](#).
- [95] A. Sesana, “Prospects for Multiband Gravitational-Wave Astronomy after GW150914,” *Phys. Rev. Lett.* **116** (2016) no. 23, 231102, [arXiv:1602.06951 \[gr-qc\]](#).
- [96] S. Marsat, J. G. Baker, and T. Dal Canton, “Exploring the Bayesian parameter estimation of binary black holes with LISA,” *Phys. Rev. D* **103** (2021) no. 8, 083011, [arXiv:2003.00357 \[gr-qc\]](#).
- [97] A. Toubiana, S. Marsat, S. Babak, J. Baker, and T. Dal Canton, “Parameter estimation of stellar-mass black hole binaries with LISA,” *Phys. Rev. D* **102** (2020) 124037, [arXiv:2007.08544 \[gr-qc\]](#).
- [98] A. Klein *et al.*, “The last three years: multiband gravitational-wave observations of stellar-mass binary black holes,” [arXiv:2204.03423 \[astro-ph.HE\]](#).
- [99] T. Baker, E. Barausse, A. Chen, C. de Rham, M. Pieroni, and G. Tasinato, “Testing gravitational wave propagation with multiband detections,” [arXiv:2209.14398 \[gr-qc\]](#).
- [100] A. Buonanno, B. Iyer, E. Ochsner, Y. Pan, and B. S. Sathyaprakash, “Comparison of post-Newtonian templates for compact binary inspiral signals in gravitational-wave detectors,” *Phys. Rev. D* **80** (2009) 084043, [arXiv:0907.0700 \[gr-qc\]](#).
- [101] LIGO Scientific Collaboration, “LIGO Algorithm Library - LALSuite.” Free software (gpl), 2018.
- [102] J. M. Ezquiaga, W. Hu, M. Lagos, M.-X. Lin, and F. Xu, “Modified gravitational wave propagation with higher modes and its degeneracies with lensing,” [arXiv:2203.13252 \[gr-qc\]](#).
- [103] **LIGO Scientific, Virgo** Collaboration, B. P. Abbott *et al.*, “Tests of General Relativity with GW170817,” *Phys. Rev. Lett.* **123** (2019) no. 1, 011102, [arXiv:1811.00364 \[gr-qc\]](#).
- [104] L. Lindblom, B. J. Owen, and D. A. Brown, “Model Waveform Accuracy Standards for Gravitational Wave Data Analysis,” *Phys. Rev. D* **78** (2008) 124020, [arXiv:0809.3844 \[gr-qc\]](#).
- [105] R. Abbott *et al.*, “Open data from the first and second observing runs of Advanced LIGO and Advanced Virgo,” *SoftwareX* **13** (2021) 100658, [arXiv:1912.11716 \[gr-qc\]](#).
- [106] A. H. Nitz, T. Dent, G. S. Davies, S. Kumar, C. D. Capano, I. Harry, S. Mozzon, L. Nuttall, A. Lundgren, and M. Tápai, “2-OGC: Open Gravitational-wave Catalog of binary mergers from analysis of public Advanced LIGO and Virgo data,” *Astrophys. J.* **891** (2020) 123, [arXiv:1910.05331 \[astro-ph.HE\]](#).
- [107] M. Cantiello *et al.*, “A Precise Distance to the Host Galaxy of the Binary Neutron Star Merger GW170817 Using Surface Brightness Fluctuations,” *Astrophys. J. Lett.* **854** (2018) no. 2, L31, [arXiv:1801.06080 \[astro-ph.GA\]](#).
- [108] D. A. Brown, I. Harry, A. Lundgren, and A. H. Nitz, “Detecting binary neutron star systems with spin in advanced gravitational-wave detectors,” *Phys. Rev. D* **86** (2012) 084017, [arXiv:1207.6406 \[gr-qc\]](#).
- [109] D. Foreman-Mackey, D. W. Hogg, D. Lang, and J. Goodman, “emcee: The MCMC Hammer,” *Publ. Astron. Soc. Pac.* **125** (2013) 306–312, [arXiv:1202.3665 \[astro-ph.IM\]](#).
- [110] C. M. Biwer, C. D. Capano, S. De, M. Cabero, D. A. Brown, A. H. Nitz, and V. Raymond, “PyCBC Inference: A Python-based parameter estimation toolkit for compact binary coalescence signals,” *Publ. Astron. Soc. Pac.* **131** (2019) no. 996, 024503, [arXiv:1807.10312 \[astro-ph.IM\]](#).
- [111] **LIGO Scientific, VIRGO** Collaboration, B. P. Abbott *et al.*, “GW170104: Observation of a 50-Solar-Mass Binary Black Hole Coalescence at Redshift 0.2,” *Phys. Rev. Lett.* **118** (2017) no. 22, 221101, [arXiv:1706.01812 \[gr-qc\]](#).

- [Erratum: Phys.Rev.Lett. 121, 129901 (2018)].
- [112] **LIGO Scientific, Virgo** Collaboration, B. P. Abbott *et al.*, “Tests of General Relativity with the Binary Black Hole Signals from the LIGO-Virgo Catalog GWTC-1,” *Phys. Rev. D* **100** (2019) no. 10, 104036, [arXiv:1903.04467](#) [gr-qc].
- [113] **LIGO Scientific, Virgo** Collaboration, R. Abbott *et al.*, “Tests of general relativity with binary black holes from the second LIGO-Virgo gravitational-wave transient catalog,” *Phys. Rev. D* **103** (2021) no. 12, 122002, [arXiv:2010.14529](#) [gr-qc].
- [114] **LIGO Scientific, VIRGO, KAGRA** Collaboration, R. Abbott *et al.*, “Tests of General Relativity with GWTC-3,” [arXiv:2112.06861](#) [gr-qc].
- [115] A. Klein *et al.*, “Science with the space-based interferometer eLISA: Supermassive black hole binaries,” *Phys. Rev. D* **93** (2016) no. 2, 024003, [arXiv:1511.05581](#) [gr-qc].
- [116] M. L. Katz and S. L. Larson, “Evaluating Black Hole Detectability with LISA,” *Mon. Not. Roy. Astron. Soc.* **483** (2019) no. 3, 3108–3118, [arXiv:1807.02511](#) [gr-qc].
- [117] **AEDGE** Collaboration, Y. A. El-Neaj *et al.*, “AEDGE: Atomic Experiment for Dark Matter and Gravity Exploration in Space,” *EPJ Quant. Technol.* **7** (2020) 6, [arXiv:1908.00802](#) [gr-qc].
- [118] J. M. Martín-García, “xAct 2002-2014,” <http://www.xact.es/>.
- [119] A. Nitz *et al.*, “PyCBC: v2.0.3 release of PyCBC.” Zenodo, May, 2022. <https://doi.org/10.5281/zenodo.6583784>.
- [120] C. R. Harris *et al.*, “Array programming with NumPy,” *Nature* **585** (2020) no. 7825, 357–362, [arXiv:2006.10256](#) [cs.MS].
- [121] P. Virtanen *et al.*, “SciPy 1.0—Fundamental Algorithms for Scientific Computing in Python,” *Nature Meth.* **17** (2020) 261, [arXiv:1907.10121](#) [cs.MS].
- [122] M. Maggiore, *Gravitational Waves. Vol. 1: Theory and Experiments*. Oxford Master Series in Physics. Oxford University Press, 2007.